JGR Earth Surface

RESEARCH ARTICLE
10.1029/2023JF007284

Geochemical Weathering Variability in High Latitude Watersheds of the Gulf of Alaska

J. Jenckes[1], S. Muñoz[2,3], D. E. Ibarra[2,3], D. F. Boutt[4], and L. A. Munk[5]

[1]Department of Chemistry, University of Alaska Anchorage, Anchorage, AK, USA, [2]Department of Earth, Environmental and Planetary Sciences, Brown University, Providence, RI, USA, [3]Institute at Brown for Environment and Society, Brown University, Providence, RI, USA, [4]Department of Geosciences, University of Massachusetts Amherst, Amherst, MA, USA, [5]Department of Geological Sciences, University of Alaska Anchorage, Anchorage, AK, USA

Key Points:

- Carbonate weathering dominates the solute flux of chemical weathering derived products
- Weathering by sulfuric acid is elevated in glacierized basins compared with non-glacierized
- Silicate weathering is strongly controlled by glacier coverage, relief, and air temperature

Supporting Information:

Supporting Information may be found in the online version of this article.

Correspondence to:

J. Jenckes,
jjenckes2@alaska.edu

Citation:

Jenckes, J., Muñoz, S., Ibarra, D. E., Boutt, D. F., & Munk, L. A. (2024). Geochemical weathering variability in high latitude watersheds of the Gulf of Alaska. *Journal of Geophysical Research: Earth Surface*, *129*, e2023JF007284. https://doi.org/10.1029/2023JF007284

Received 2 JUN 2023
Accepted 14 FEB 2024

Author Contributions:

Conceptualization: S. Muñoz, D. E. Ibarra, D. F. Boutt, L. A. Munk
Funding acquisition: L. A. Munk
Investigation: S. Muñoz
Methodology: S. Muñoz, D. E. Ibarra
Writing – review & editing: S. Muñoz, D. E. Ibarra, D. F. Boutt, L. A. Munk

Abstract High latitude regions across the globe are undergoing severe modifications due to changing climate. A high latitude region of concern is the Gulf of Alaska (GoA), where these changes in hydroclimate undoubtedly affect the hydrogeochemistry of freshwater discharging to the nearshore ecosystems of the region. To fill the knowledge gap of our understanding of freshwater stream geochemistry with the GoA, we compile stream water chemistry data from 162 stream sites across the region. With an inverse model, we estimate fractional contributions to solute fluxes from weathering of silicate, carbonate, and sulfide minerals, and precipitation. We assess weathering rates across the region and compare them against global river yields. The median fractional contribution of carbonate weathering to total weathering products is 78% across all stream sites; however, there are several streams where silicate weathering is a dominant source of solutes. Weathering by sulfuric acid is elevated in glacierized watersheds. Finally, cation weathering rates are lower in GoA streams compared to the world's largest rivers; however, weathering rates are similar when compared to a global dataset of glacier fed streams. We suggest that hydrologic changes driven by glacier ice loss and increased precipitation will alter river water quality and chemical weathering regimes such that silicate weathering may become a more important source of solutes and sulfide oxidation may decrease. This contribution provides a platform to build from for future investigations into changes to stream water chemistry in the region and other high latitude watersheds.

Plain Language Summary The Gulf of Alaska (GoA) is a region in high latitudes that is experiencing significant changes due to climate change. These changes affect the chemistry of freshwater streams that flow into the nearby ecosystems. We collected data on the chemistry of stream water from 162 sites in the region. Using a model to estimate where the different solutes in the water come from, such as minerals and rain. We found that carbonate minerals are the main source of solutes in most streams, but in some streams, silicate minerals are more important. Glaciers in the region cause higher levels of sulfide weathering. Compared to the largest rivers in the world, the rates at which minerals are released in the GoA streams are lower, but similar to streams fed by glaciers worldwide. We predict that as glaciers melt and precipitation increases, the chemistry of the streams will change, with more silicate minerals being released and less weathering of sulfide minerals. This study provides a foundation for future research on the effects of climate change on stream water chemistry in the region and other high latitude areas.

1. Introduction

Global climate change has resulted in the accelerated melting of the world's glaciers. High-latitude regions, specifically, are warming two to four times faster than the rest of the planet (IPCC, 2022), leading to increased discharge of freshwater derived from glacier melt (Beamer et al., 2017; Young et al., 2021). Additionally, by the end of the century, precipitation as rain is predicted to increase especially during the fall and winter months, further increasing freshwater export. The Gulf of Alaska (GoA) region is a culturally, environmentally, and economically important high-latitude region that supports a diverse ecological ecosystem and both commercial and subsistence fisheries and other maricultural activities (Johnson et al., 2019; Schoen et al., 2017). Within the GoA region, glacierized watersheds supply geochemically (Jenckes et al., 2022, 2023) and biogeochemically unique sources of freshwater that support nearshore ecosystems (Fellman, Hood, et al., 2014; Hood & Berner, 2009; Hood et al., 2020). The alteration of hydrologic regimes and loss of glacier ice in the GoA has unknown implications for the future fluxes of the major, minor and trace elements and SiO_2 to the nearshore

ecosystem. Characterizing current geochemical processes within the GoA that control stream solute loads is an important step in building an understanding of how future climate changes will alter freshwater and solute fluxes to the GoA.

The chemistry of stream water within glacierized basins has distinct chemistry compared to non-glacier fed streams (Anderson et al., 1997; Torres et al., 2017), such that globally, river water major elemental concentrations in glacierized catchments are lower. However, solute yields within glacierized catchments are similar to those without glaciers. Chemical weathering of carbonate and silicate minerals is the primary driver of variability in the concentrations of the major elements within natural waters and there are distinct reaction mechanisms between silicate and carbonate weathering (Calmels et al., 2007; Colbourn et al., 2015; Torres et al., 2014; Winnick et al., 2017). Within the common framework describing weathering reactions, carbonate minerals dissolve congruently by carbonic acid resulting in the complete dissolution of the mineral, while silicate weathering occurs incongruently by carbonic acid. The incongruent weathering of silicates provides cations and alkalinity to solution and forms secondary minerals that can contribute to sediment and soil formation.

In a transport limited regime, the erosion rate is low inhibiting the supply of fresh mineral surfaces. At high levels of erosion, chemical weathering is kinetically limited because the supply of un-weathered material outpaces the kinetics of silicate chemical weathering (West et al., 2005). Chemical weathering in high alpine regions is generally suppressed, primarily due to low temperatures and a lack of vegetation and soil. High elevation glaciers, however, promote physical weathering many times over compared to non-glacierized basins, which can act to enhance chemical weathering. Glacierized basins, however, have been shown to have similar chemical weathering fluxes as non-glacierized basins (Anderson et al., 1997). The weathering products of Ca silicate weathering are Ca^{2+} and alkalinity, which are transported to the ocean where they combine to from $CaCO_3$ thus acting as a sink for C and lowing atmospheric CO_2. Thus, modeling efforts of weathering rates are primarily focused on elucidating CO_2 drawdown by silicate weathering by carbonic acid.

Besides carbonic acid, sulfuric acid produced by the oxidation of sulfides (Equation S5 in Supporting Information S1) is an extremely important pathway for chemical weathering. Sulfuric acid dissolves both silicate and carbonate minerals though it preferentially dissolves carbonates over silicates at a rate of 5:1 (Tranter, Huybrechts, et al., 2002). Tranter, Huybrechts, et al. (2002) and Tranter, Sharp, et al. (2002) have shown that the role of sulfide oxidation in glacierized watersheds is an extremely important pathway for controlling the chemistry of the dissolved load transported downstream. Sulfide oxidation coupled to carbonate dissolution (Equation S6 in Supporting Information S1) alters water quality by changing the alkalinity budgets delivered to the oceans as well as liberating ions during the process.

Glaciers modify the relative proportion of the different chemical weathering reactions regardless of the dominant underlying lithology of the basin (Hindshaw et al., 2016; Raiswell, 1984; Tranter & Wadham, 2003). Due to the decreased water temperatures in glacierized basins, silicate weathering is reduced compared to a non-glacierized basin (Anderson, 2005; Anderson et al., 1997). In most cases, chemical weathering of carbonates dominates the sourcing of solutes in glacierized basins even if the primary lithology is silicates. Furthermore, sulfide oxidation maybe enhanced in glacierized basins, likely due to the increased physical erosion supplying a constant source of fresh un-weathered material (Torres et al., 2017; Tranter, Sharp, et al., 2002; Tranter & Wadham, 2003). Even in the absence of glacier coverage, sulfide weathering can be elevated in a basin subject to high rates of erosion due to the relief, slope, or climate (Calmels et al., 2007; Torres et al., 2014, 2016).

There has been limited attention given to the weathering regimes that control the water chemistry of rivers within the GoA watershed. Work by Brennan et al. (2014) utilized grab samples, primarily taken in midsummer to early fall, from the major rivers throughout Alaska to broadly describe chemical weathering regimes. Their work illustrated that in general, carbonate weathering is the dominant source of solutes to streams in the central GoA region. Additionally, Jenckes et al. (2022) showed, using molar ratios of Ca^{2+}, HCO_3^-, and SiO_2, that carbonate weathering is dominant across the GoA. However, these studies lack: (a) a description of the contribution of precipitation to solute loads, (b) an evaluation of the weathering done by carbonic or sulfuric acid, and (c) spatial resolution to capture chemical weathering across a range of glacier coverage, lithology, and elevations. These are important to define due to the influence they exert on the river water chemistry and to conceptualize how they may be altered under future climate conditions. The primary objective of this work is to show that as glaciers continue to recede and precipitation regimes change throughout the GoA, geochemical weathering is expected to shift such that silicate weathering may become an important control on river

chemistry and sulfide oxidation may decline, which will further alter the water quality of freshwater discharge to near shore ecosystems.

Therefore, it is important to distinguish the different sources of chemical weathering products, specifically, defining the contributions to solute flux from silicate and carbonate minerals via carbonic or sulfuric acid weathering. The work presented here is an effort to fill knowledge gaps in our understanding of solute sources and fluxes to the GoA and test hypotheses on how river water chemistry may change as cryosphere-influenced watersheds in the GoA continue to evolve. Our approach utilizes stream chemistry from 152 USGS stream sites across the GoA. Additionally, we supplement the dataset, with high resolution seasonal and interannual data from the 10 stream sites in Kachemak Bay and Lynn Canal, characterized by Jenckes et al. (2023). We first summarize the average uncorrected for precipitation solute concentrations and fluxes. Next, by way of an inversion model, MEANDIR (Kemeny & Torres, 2021), we show the fractional contributions of precipitation, carbonate, silicate, and pyrite to stream solute fluxes. We then show the variability of weathering done by sulfuric acid versus carbonic acid weathering throughout the GoA. Finally, we discuss how watershed characteristics affect the fractional contributions from carbonate and silicate minerals, and weathering yields and provide hypotheses on how these may change under future climate conditions. Overall, this work aims to provide valuable context to current and future studies that are focused on the linkage between terrestrial and ocean ecosystems.

This work is accompanied by a companion manuscript by Muñoz et al. (2024). Within this manuscript, we aim to describe the broad geochemical weathering processes that contribute to the observed river water chemistry across the GoA. The companion piece uses a subset of watersheds within the GoA described by Jenckes et al. (2023) to provide a more detailed and targeted analysis of geochemical weathering processes. In this study, we use a broad definition of end-members and do not include any isotope system to aid in exploring secondary mineral formations. Additionally, Muñoz et al. (2024) provide detailed concentration-discharge and fractional-discharge relationship analysis and calculate CO_2 consumption. These two manuscripts, taken together, provide two complimentary perspectives of the geochemical weathering regimes within the GoA region.

2. Study Region

The GoA watershed covers ~420,000 km^2 from the Western Cook Inlet, north to the Alaska Range and east to the Wrangell St. Elias Mountains of the central coastal region and the Coast Mountains in Southeast Alaska (Figures 1a and 1b). The seven sub-regions comprise many different hydroclimates from perhumid in the Southeast to subarctic in the northern regions. The seven regions, delineated by Neal et al. (2010) (Figure 1b) are from west to east Western Cook Inlet/Kodiak (WCI), Knik Arm/Kenai Peninsula (KP), Susitna River (SR), Prince William Sound (PWS), Copper River (CR), Central Coast (CC), and Southeast (SE).

2.1. Hydroclimate

The hydroclimate of the GoA has been described in detail; however, we provide a general overview (Beamer et al., 2017; Curran & Biles, 2021; Jenckes et al., 2022; Neal et al., 2010; Sergeant et al., 2020). Seasonal precipitation varies widely both seasonally and regionally across the GoA. Precipitation is highest in the SE, CC, and PWS regions with most of the precipitation occurring in the fall and winter. Variability in precipitation patterns is driven by the dominant storm track trajectories in the GoA and orographic precipitation patterns.

Across the GoA, seasonal river runoff patterns are primarily driven by precipitation and glaciers. Streams within glacier fed watersheds generally have peak discharge in July and August. Non-glacierfed streams typically have two distinct peaks in discharge with the first in spring driven by snowmelt and the second in the fall induced by rain events.

2.2. Geology

The geologic history of the GoA region is complex being characterized by multiple deformation events associated with collision, subduction, and metamorphism. The coastal margin, approximately 0–40 km inland, consists of alluvium and glacierized lowlands. Beyond this margin are the Kenai, Chugach, and Saint Elias of the South-central and CC regions and the Fairweather Range and Coast Mountains in the southeast. The average elevation of these ranges is approximately 2,000 m, with several peaks reaching above 5,000 m. Further inland, the Alaska range makes up the northern portion of the SR region.

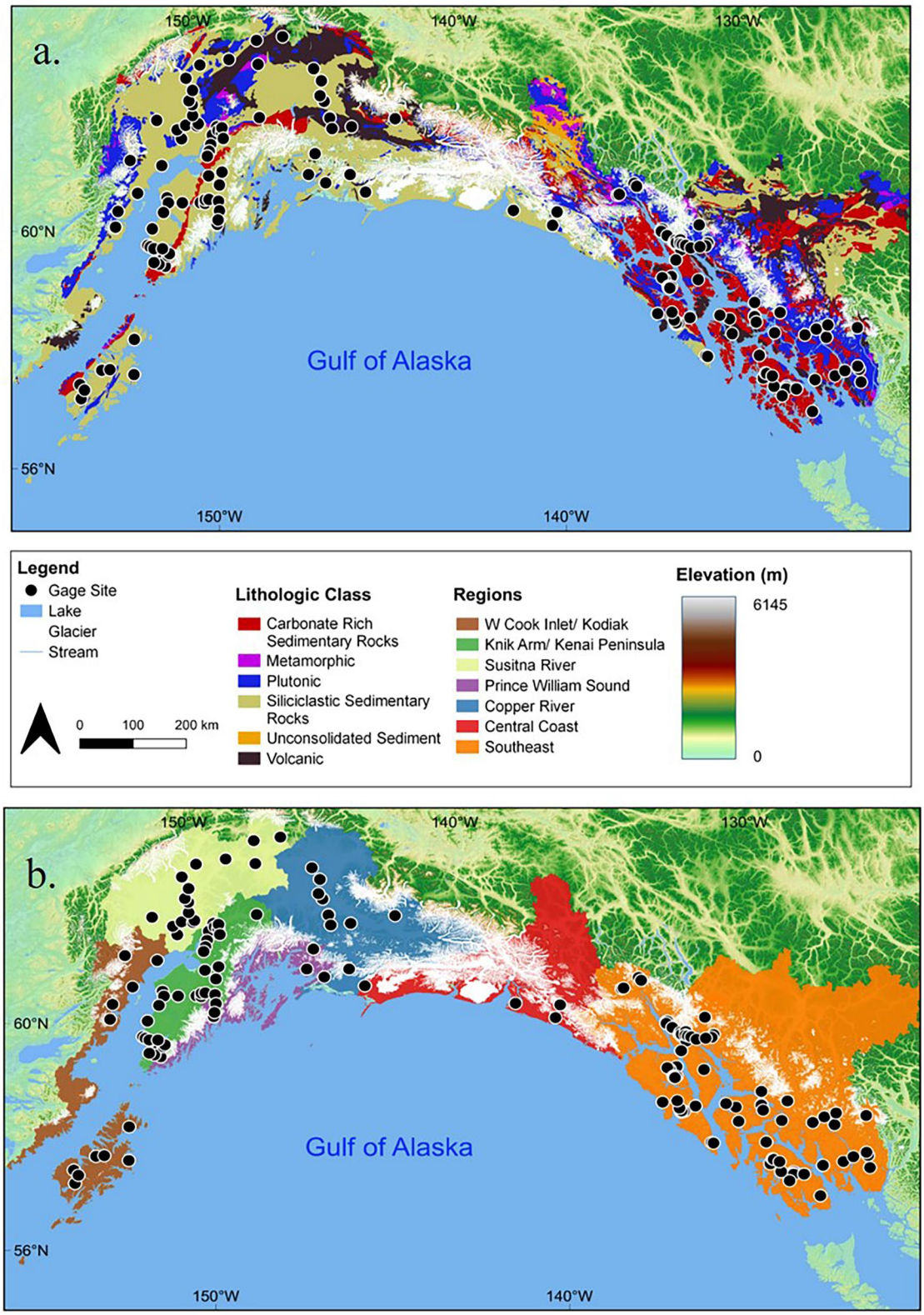

Figure 1. Study area extent of the Gulf of Alaska (GoA) watershed with the selected gage sites. Spatial distribution of lithologic classes (Hartmann & Moosdorf, 2012) across the GoA (a) and the seven distinct hydroclimate regions of the GoA (b).

Across the GoA region, the geology spans a wide variety of lithologies. There are a few distinctions that can provide context for the chemical weathering regimes we observe. In the SR and KP regions of GoA, meta-sedimentary lithologies are prevalent. Comparatively, within the CR, CC, and SE regions, there is a greater occurrence of volcanic and plutonic lithologies. Across the GoA, there are many ore deposits and associated mineralized zones that contain sulfides.

2.2.1. Southern Margin of Alaska

The geology of the region has been described in detail by Bradley et al. (1999), Kusky and Bradley (1999), and Wilson et al. (2015); here, we provide a brief distillation of those resources. The southern Alaska margin is composed of the Southern Margin composite terrane that includes the Prince William and Chugach Terranes, and the Wrangellia composite terrane. Similar to other tectonic terranes in Alaska, the southern margin of Alaska is an amalgamation of accreted terranes. The formation of this region began in the Mesozoic and continues to be shaped by ongoing tectonic processes. Within the Southcentral region, the geology is defined by the Chugach-Prince William (CPW) composite terrane, which is a Mesozoic accretionary complex. Approximately 2,200 km of the southern margin of Alaska is composed of the CPW. The CPW is primarily a trench-fill turbidite sequence that is overlapped by a sequence of pillow basalts and associated sediments. Once accreted, the CPW was intruded by the plutons, which range in age from 61 Ma to 50 Ma, of the Sanak-Baranof near trench belt. The CPW started to be uplifted in the early Miocene due to the subduction of the Pacific plate and Yakutat terrane. Until the Pleistocene glaciation began, the CPW most likely resembled a large plateau incised by V-shaped valleys. The Pleistocene glaciation sculpted the region as we know it today.

2.2.2. Southeast Alaska

Southeast Alaska is characterized by an archipelago and is heavily glaciated and forested. The area is underlain by complex assemblages of rocks that are cut by faults. Regional lithology is characterized by stratified and intrusive rocks of the Coast Mountains batholith. Stratified rocks include graywacke and mafic-intermediate volcanic rocks that range from pre-Jurassic to upper Cretaceous that flank the Coast Mountains batholith. Meta-stratified rocks occur within the Coast Mountains batholith itself and consist of pre-Tertiary schist, gneiss and marble. The intrusive rocks of the Coast Mountains batholith range from Early Cretaceous to Paleocene. These intrusive rocks include sheet like masses of hornblende tonalite and quartz diorite. To the east of the tonalitic bodies are Paleocene batholiths of granodiorite. Within the Southeast region, most of the glacial ice occurs on top of the intrusive bodies, while the streams and rivers flow through the stratified rocks that flank the Coast Mountains (Wilson et al., 2015).

3. Methods

3.1. Hydrochemical Data Compilation

The river chemistry data was compiled from data queried from the USGS NWIS and data from Jenckes et al. (2023) (see Supporting Information S1 for details). The USGS NWIS was queried to obtain all stream sites within the GoA that had concentration data for Ca, Mg, Na, K, Cl, SO_4, HCO_3, SiO_2 and discharge data. We queried the NWIS database so that only samples in which HCO_3 concentrations were derived from alkalinity determined by titration methods were returned. For samples collected by Jenckes et al. (2023) HCO_3 was calculated from alkalinity concentrations obtained by titration methods. In this study, we use HCO_3 concentrations primarily for graphical representation of the variability in water chemistry across our chosen study sites. We do not use HCO_3 within our model design (see Section 3.3 for further details). For precipitation data, we compiled data from three (AK97, AK03, and AK07) National Atmospheric Deposition Program (NADP) sites. The NADP sites are situated at the north, west, and east extremes of the GoA region. We supplement these data with precipitation chemistry collected by Jenckes et al. (2023) within the southern KP region. Quality control for river water samples included removing any samples where the charge of the anions (SO_4 and Cl) exceeded the charge of the cations (Ca, Mg, Na, K; see Cole et al., 2022). This resulted in a dataset with 3,210 unique river water samples in 162 unique stream gage sites across the GoA (Table S1). No quality control was applied to the precipitation sample dataset (similar to Cole et al., 2022).

The resulting stream chemistry dataset gathered from the USGS and Jenckes et al. (2023) spans a timeframe from 1949 to 2021 (see Table S4 for details). Across the sites, there was variability in the number of sampling efforts

ranging from 237 samples to one sample. Across the GoA, there is also considerable variability in the number of sites per region as well as sites with or without glaciers. Of the sites we chose for our investigation, the SE region contains the most historical and active streams site with a total of 80 gage locations, while the CC region contains four sites. Figure S1 in Supporting Information S1 provides a breakdown of sites per region and is grouped by glacier coverage.

Additionally, in Table S4, we provide the percentage of sampling events that occurred within each season. In this case, we use the meteorological definition of the four seasons. Figure S2 in Supporting Information S1 illustrates the fraction of sampling events that occurred in each season grouped by the seven primary regions of the GoA. Though there are individual sites that may not have data for each season, we show that on a regional level most samples were obtained during the spring, summer, and fall months. There may be limited samples during the winter months; however, throughout the GoA region, winter stream flow is a relatively small fraction of the annual discharge (Beamer et al., 2016). Therefore, within our compiled dataset we do observe a bias in data collection during the spring, summer, and fall; however, we view this sampling bias as acceptable due to the seasonal nature of stream and river discharge in the GoA watersheds.

3.2. Watershed Characteristics

For watershed boundaries of the 152 USGS stream sites with requisite chemistry data, we use the watersheds delineated by Curran and Biles (2021). When watershed boundaries were not available, we used the R package *whitebox* (Lindsay, 2016) to delineate watershed boundaries. For the remaining 10 watersheds, we use the watershed characterization from Jenckes et al. (2023). Watershed characteristics were calculated in a fashion similar to Jenckes et al. (2022); here we provide a general overview. Watershed characteristics were calculated using five different datasets: landcover (CCRS, 2015) at 30 m resolution, lithology classification (Hartmann & Moosdorf, 2012), elevation statistics at 30 m resolution (mean elevation, relief, mean slope, and mean aspect (Tadono et al., 2014)), glacial coverage (RGI Consortium, 2017) and climate from the DAYMET climate product at a resolution of 800 m (Thornton et al., 2020). Each dataset was clipped using watershed boundaries and the specific parameters were grouped and calculated. All calculated watershed characteristics are tabulated and can be found in Table S2.

3.3. Inversion Model

This work is based on many years of previous studies that attempt to explain the weathering processes that control the chemical composition of streams and rivers. Initial key work done by Garrels and Mackenzie (1967) and later Meybeck (1987) utilized mineral mass balance and specific lithology weathering, respectively, to identify appropriate solute sources observed in river water. An inversion modeling approach (Burke et al., 2018; Gaillardet et al., 1999; Moon et al., 2014; Négrel et al., 1993) uses dissolved concentrations of major or trace elements and often isotopic ratios in river water to describe the mineralogic or lithologic origin of the solute. Most studies within this realm utilize a Monte Carlo approach to vary the end-member composition to explore the full range of results. In order to create a unified and customizable modeling process Kemeny and Torres (2021) developed MEANDIR, which brings together the decades of work by themselves and other researchers. MEANDIR is a group of MATLAB scripts that allows for the inversion of dissolved river chemistry that utilizes a Monte Carlo scheme for the propagation of uncertainty.

The MEANDIR scripts allow for the determination of fractional contributions to solute flux from user defined end-members. For our study, we use $\Sigma^{\pm}$ normalized molar ratios of Ca, Mg, Na, SO_4, and Cl to solve for the fractional end-member contributions from silicate, carbonate, precipitation, and pyrite. This is achieved by solving the following equation (Cole et al., 2022; Kemeny & Torres, 2021):

$$\left(\frac{X}{\Sigma^{\pm}}\right)_{river} = \sum_{i=1}^{n} f_i \left(\frac{X}{\Sigma^{\pm}}\right)_i$$

where $\Sigma^{\pm}$ is the sum of Ca, Mg, Na and SO_4 and $X/\Sigma^{\pm}_{river}$ is the molar ratio of $Ca/\Sigma^{\pm}$, $Mg/\Sigma^{\pm}$, $Na/\Sigma^{\pm}$, $SO_4/\Sigma^{\pm}$ and $Cl/\Sigma^{\pm}$ of each river sample and $(X/\Sigma^{\pm})_i$ is the molar ratio for the given end-member. In our inversion model, we do not use HCO_3. Bicarbonate concentration is not only regulated by weathering reactions but also can be altered by exchanges with the atmosphere and biological respiration (Quay et al., 1995; Raymond et al., 2013). We use a set

Table 1
Endmember Ratios Used for MEANDIR Simulations

		Carbonate	Precipitation	Pyrite	Silicate
$Ca/\Sigma^{\pm}$	Min	0.317	0.03	0	0.039
$Ca/\Sigma^{\pm}$	Max	1.000	0.86	0	0.591
$Mg/\Sigma^{\pm}$	Min	0.000	0.01	0	0.000
$Mg/\Sigma^{\pm}$	Max	0.675	0.28	0	0.466
$Na/\Sigma^{\pm}$	Min	0.000	0.02	0	0.209
$Na/\Sigma^{\pm}$	Max	0.000	0.83	0	0.677
$Cl/\Sigma^{\pm}$	Min	0.000	0.03	0	0.000
$Cl/\Sigma^{\pm}$	Max	0.000	1.2	0	0.000
$SO_4/\Sigma^{\pm}$	Min	0.000	0.03	1	0.000
$SO_4/\Sigma^{\pm}$	Max	0.003	0.87	1	0.000

of end-member values for silicate, carbonate, and pyrite compiled by Kemeny and Torres (2021), which are from a global compilation of silicate and carbonate chemistry that represent a broad range of these minerals found throughout the world. This method has been effectively used in previous studies (e.g., Gaillardet et al., 1999; Kang et al., 2022), which investigate chemical weathering across large study areas. For the purpose of this study, we do not use an evaporite end-member. Evaporite deposits are extremely minor mineral types throughout the GoA region. There are known evaporite occurrences within the Triassic Chitisone Limestone that occurs in the Wrangell Mountains of the CC region (Armstrong & MacKevett, 1977). Additionally, there are gypsiferous deposits at Sheep Mountain situated in the northern part of the KP region (Eckhart, 1951). Throughout the rest of the GoA region, evaporites are not reported and therefore provide relatively minor contributions to the overall river chemistry, especially at the resolution of this study. The minimum and maximum values of our selected end-members used in the MEANDIR simulations are given in Table 1. For the precipitation end-member, we use the data compiled from the NADP sites described above and take the minimum and maximum values from the range of samples. In our model, precipitation is the only endmember which contributes Cl^- (see Table 1 for endmember distributions).

MEANDIR uses a Monte-Carlo approach to sample a complete range of endmember compositions. In our model simulations, endmember ratios are generated randomly from the defined range with an assumed uniform distribution. For each unique stream sample (n = 3,210) 100,000 simulations were completed. Of those 100,000 reconstructed values, we chose to keep 200 generated values that are within ±15% of the observed river value. As discussed by Cole et al. (2022) and Kemeny and Torres (2021), this approach accounts for analytical uncertainty and provides a reliable way of removing poor-fitting simulation results. At the end of the inversion, each stream sample contains 200 accepted results for each of the modeled parameters.

3.4. Post-Simulation Calculations

Once the mixing fractions are calculated, MEANDIR can provide two additional results: the fraction of weathering products sourced from carbonates and the fraction of weathering done with H_2SO_4. Keeping with the conventions imparted by Kemeny and Torres (2021), the variable R is the fraction of weathering products sourced from carbonates and the variable Z is the fraction of weathering done with H_2SO_4 (sulfuric acid). The variables R and Z are calculated post inversions since they rely on the calculated mixing fractions. The R value is calculated by the equation (Kemeny & Torres, 2021):

$$R = \frac{\Sigma^{\pm}_{\text{carbonate}}}{\Sigma^{\pm}_{\text{carbonate}} + \Sigma^{\pm}_{\text{silicate}}}$$

The second parameter, Z, is defined as the fraction of weathering done by sulfuric acid (Kemeny et al., 2021; Kemeny & Torres, 2021) and defined by the equation:

$$Z = \frac{SO_4^{2-}{}_{\text{pyrite}}}{\Sigma^{\pm}_{\text{carbonate}} + \Sigma^{\pm}_{\text{silicate}}}$$

In our study, we assume that the sulfuric acid is generated from the oxidation of pyrite (FeS_2). Within the framework of this study, our motivation for the calculating the variables R and Z is primarily to investigate the primary controls on river water chemistry throughout the GoA. Proportions of weathering done by sulfuric or carbonic acid or the fraction of weathering products from carbonate weathering versus silicate weathering across a wide spectrum of watersheds can provide an opportunity to investigate large scale processes that ultimately control the river water quality and potential implications for the global carbon cycle.

In summary, for this study, we use the MEANDIR framework to model the fractional contributions of silicate, carbonate, precipitation and pyrite to river water cations and anion loads. Additionally, MEANDIR calculates

R, the fractional contribution of cations from carbonate weathering and *Z*, the fractional contribution to weathering by sulfuric acid.

3.5. Data Analysis

3.5.1. MEANDIR Analysis

In this study, we focus on the illustrating the results MEANDIR calculated values of the fractional contributions to the dissolved solute load from silicate, carbonate, and precipitation along the *R* and *Z* variables. In order to obtain a single median value and corresponding 25th and 75th percentiles to represent error for the each of the fractional weathering components at each stream site, we calculate the median using all accepted simulation results across all samples for an individual stream site.

3.5.2. Flux Calculations

To calculate the fluxes of the solutes across the GoA, we first calculated the average concentration at each stream site for the chosen solute. We then calculate the average discharge measured at each gage site, utilizing the timeseries of discharge data collected at each USGS site or data collected by Jenckes et al. (2023). The fluxes are a product of the average concentration and average discharge converted to a yearly flux. Average discharge used is provided in Table S2.

3.5.3. Correlation Data Analysis

All calculated watershed characteristics and median fractional contributions from each of the endmembers were entered into a matrix (Table S2). With this matrix, we calculated a Pearson coefficient correlation matrix for each combination of parameters (Table S3). With these calculated coefficients, we found combinations of parameters with the best *r* values and explored these relationships with the creation of a heatmap (Figure 8) using a subset of watershed characteristics and modeled weathering products.

3.6. Model Uncertainty

Across the USGS stream sites there are variable amounts of stream chemistry collected at each site. The uncertainty represented by the error bars incorporates many aspects of the variations which we do not address within this study. Primarily, we do not investigate the seasonality of weathering regimes. Previous work on changes in weathering and solute concentrations (Jenckes et al., 2023; Kemeny et al., 2021) show that solute concentrations and chemical weathering regimes may vary seasonally. Furthermore, we use generalized end member definitions that do not capture all of the heterogeneity represented by the geology in the studied watersheds. The advantage of using the MEANDIR framework is the use of the Monte Carlo scheme to provide a robust representation of the possible fractional contributions from each end member. Though there is uncertainty within the model results shown in Figure 3, we attempt to make interpretations within the context of all possible results. That is to say, our interpretations of dominant weathering processes across our dataset hold true within the bounds of the model uncertainty.

3.6.1. Alternate Model Scenarios

In Supporting Information S1 document, we illustrate the results from two alternate model scenarios to explore how the original model result (results we use in throughout this study) compares to different choices in model design. In the first alternate scenario (results shown in Figure S8 in Supporting Information S1), we average the concentrations across all samples at each stream site. This results in providing the model 162 samples compared to 3,210 in the original design. In the second scenario we add HCO_3 to the model (Figure S9 in Supporting Information S1). We find that using the average concentrations of cations and anions at each sample site in the inversion model provide similar results compared to the original model scenario, though there are a handful of outliers that show poor agreement in model results (see Figure S8 in Supporting Information S1). In the second alternate modeling scenario (Figure S9 in Supporting Information S1) with the addition of HCO_3, we find good agreement between the original and alternate scenario for the majority of sample sites.

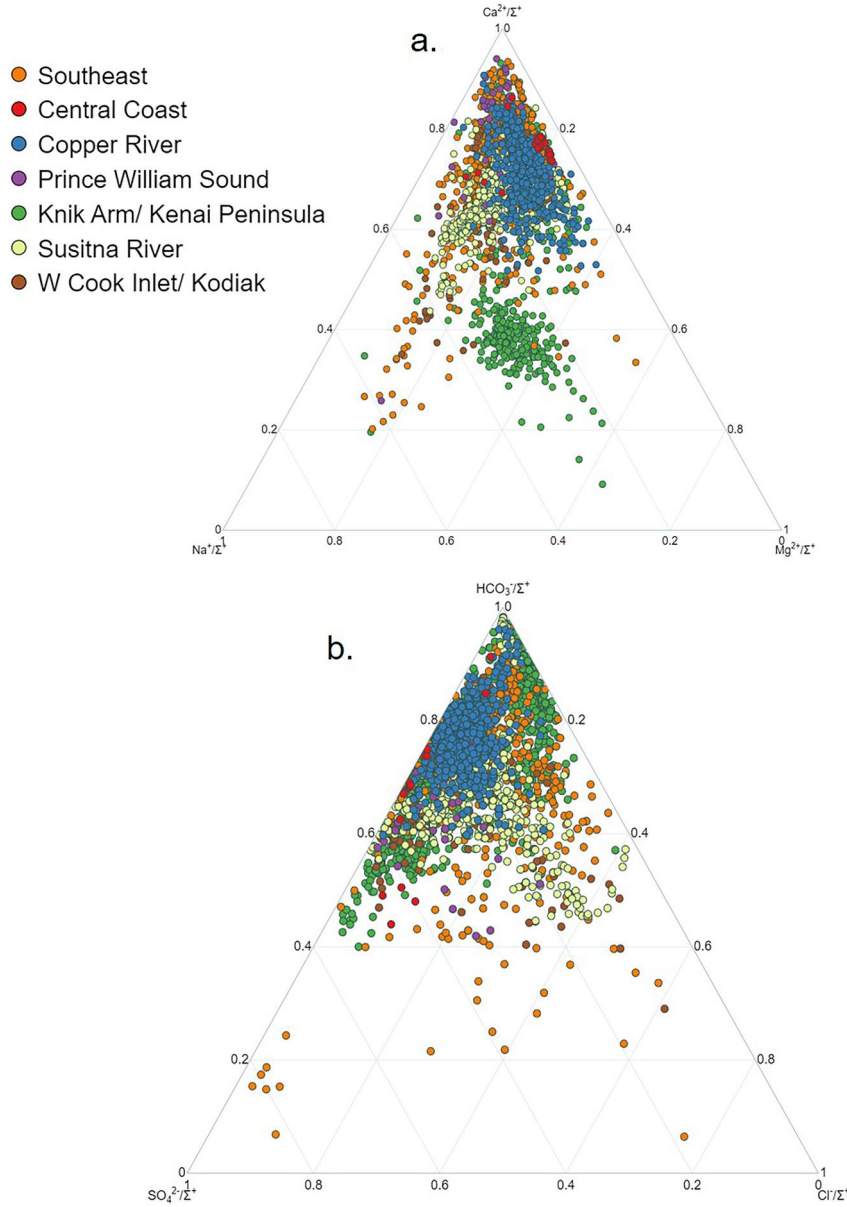

Figure 2. Ternary diagram showing the Σ^+ normalized cations (a) and anions (b) for all river samples used in the study.

4. Results

4.1. Hydrochemistry

Across the GoA regions, we find a wide distribution of the raw (not corrected for precipitation input) major ion concentrations in our compiled database; however, we do observe several features of the water chemistry that are similar across the regions (Figure 2 and Table 2). Overall Ca^{2+} is the dominant cation and HCO_3^- and SO_4^{2-} are the dominant anions. In the majority of river samples, Ca^{2+} accounts for more than 60% of Σ^+. There are several streams in the KP region that plot near the middle of the ternary diagram with elevated Na^+/Σ^+ (Figure 2). The bulk of HCO_3^-/Σ^+ values are above 60% with most of the SO_4^{2-}/Σ^+ values occurring between 15% and 35%. The CR region has the highest concentrations of major ions with the SE and WCI regions having the lowest concentrations. Average SiO_2 concentrations are highest in the KP region and lowest in the SE. Compared to global river averages (Gaillardet et al., 1999), rivers within the GoA region on average have lower overall concentrations

Table 2
Uncorrected for Precipitation Average Concentration of the Major Ions for Each Region and Divided Into Respective Glacier Coverage Categories

Region	Glacier coverage	Ca	Mg	Na	Cl	SO_4	HCO_3	SiO_2	Ca:SiO_2
		(μmol/L)							
W Cook Inlet/Kodiak	High	207	29	41	20	96	299	51	4
	Medium	177	33	49	26	75	316	80	2
	Low	129	35	85	65	44	266	69	2
	No Glacier	171	60	173	166	76	330	110	4
	Average	171	39	87	69	73	303	77	3
Susitna River	Medium	523	168	150	102	216	1,034	100	6
	Low	473	109	267	255	145	927	122	4
	No Glacier	165	56	123	76	22	439	183	1
	Average	387	111	180	144	128	800	135	4
Knik Arm/Kenai Peninsula	High	454	88	151	39	165	775	39	18
	Medium	495	115	144	71	215	865	83	7
	Low	365	73	100	57	93	712	86	4
	No Glacier	283	147	240	95	96	821	360	2
	Average	399	106	159	65	142	793	142	8
Prince William Sound	High	493	31	63	58	185	712	61	8
	Medium	429	62	113	68	110	822	74	6
	Low	255	15	61	55	78	384	36	7
	No Glacier	70	12	38	34	28	121	52	1
	Average	312	30	69	54	100	510	56	6
Copper River	Medium	571	149	208	147	179	1,147	111	6
	Low	467	127	148	83	120	1,040	103	5
	No Glacier	500	192	179	82	46	1,425	176	3
	Average	513	156	178	104	115	1,204	130	4
Central Coast	Medium	628	159	73	47	256	1,300	52	12
	Low	649	66	89	55	63	1,377	52	13
	No Glacier	198	33	107	53	124	283	88	4
	Average	492	86	90	52	148	986	64	10
Southeast	High	195	27	28	18	68	379	35	7
	Medium	239	49	54	32	80	428	55	4
	Low	346	91	80	43	101	601	68	5
	No Glacier	212	37	82	75	47	366	60	4
	Average	248	51	61	42	74	443	54	5
Global Rivers		866	475	1,315	1,370	391	1,813	133	7
Global Glacier Rivers		324	108	96	43	204	447	68	5
GoA Glacier Rivers		394	79	106	69	127	743	71	7

of the major ions. Silica concentrations from the SR, KP, and CR regions are comparable to the global river compilation, while SiO_2 concentrations in the remaining regions are much lower (Table 2).

Glacier influenced watersheds illustrate unique patterns in ion concentrations across all regions. The concentrations of Ca^{2+} are elevated within glacierized watersheds, but SiO_2 concentrations show a negative relationship with glacier coverage. In general, SO_4^{2-} concentrations are elevated in glacierized watersheds, though there is some variability in this observation across the regions. Bicarbonate concentrations are generally elevated in glacierized watersheds except for those in WCI and CR; on average, non-glacierized watersheds are elevated

Table 3
Total Uncorrected for Precipitation Flux of the Major Ions for Each Region and Glacier Coverage Category

Region	Glacier category	Ca	Mg	Na	K	SiO_2	SO_4	Cl	HCO_3
		(10^3 t/year)							
W Cook Inlet/Kodiak	High	3.67	0.31	0.41	0.12	0.63	4.08	0.32	8.05
	Medium	17.39	2.02	2.71	2.89	5.25	18.07	2.25	46.51
	Low	1.94	0.31	0.77	0.10	0.77	1.72	0.90	6.12
	No Glacier	4.46	0.74	1.29	0.23	0.94	8.21	2.89	4.07
	Average	6.13	0.84	1.37	0.64	1.61	8.43	2.24	12.52
Knik Arm/Kenai Peninsula	High	69.92	8.71	8.92	2.18	5.38	59.40	4.64	189.67
	Medium	28.61	3.59	4.46	1.89	4.49	25.30	3.39	79.80
	Low	2.23	0.28	0.35	0.06	0.34	1.48	0.33	6.57
	No Glacier	1.77	0.45	0.76	0.12	0.83	2.23	0.35	6.19
	Average	16.65	2.17	2.59	0.85	2.29	14.63	1.70	46.48
Susitna River	Medium	157.80	30.69	23.39	10.73	22.34	171.38	23.24	453.46
	Low	256.75	38.67	63.28	21.08	40.71	189.94	91.75	767.31
	No Glacier	2.27	0.46	0.93	0.27	1.76	0.86	0.89	9.37
	Average	167.77	27.33	36.88	13.14	26.14	139.99	50.22	496.66
Prince William Sound	High	22.23	0.85	1.62	2.15	1.93	19.94	2.30	48.83
	Medium	20.01	1.67	2.08	0.54	2.22	11.78	2.41	57.59
	Low	0.73	0.03	0.10	0.02	0.07	0.54	0.14	1.69
	No Glacier	0.08	0.01	0.03	0.00	0.04	0.08	0.04	0.22
	Average	10.76	0.64	0.96	0.68	1.07	8.09	1.22	27.08
Copper River	Medium	837.49	130.88	168.94	63.22	102.91	713.17	179.11	2,417.89
	Low	25.21	4.16	5.11	1.33	3.24	14.85	5.08	85.89
	No Glacier	0.25	0.06	0.05	0.01	0.06	0.06	0.03	2.38
	Average	222.04	34.82	44.81	16.47	27.36	185.73	47.32	777.14
Central Coast	Medium	874.58	131.74	59.66	64.67	51.00	858.33	68.57	2,399.35
	Low	7.32	0.45	0.58	0.24	0.41	1.70	0.55	23.64
	No Glacier	0.98	0.10	0.30	0.02	0.30	1.47	0.23	2.13
	Average	439.36	66.01	30.05	32.40	25.68	429.96	34.48	1,206.12
Southeast	High	5.97	0.53	0.54	0.78	0.87	4.82	0.59	17.14
	Medium	14.30	1.98	1.55	1.24	1.94	13.02	1.43	37.12
	Low	93.62	15.96	12.07	4.42	11.08	62.41	9.21	302.34
	No Glacier	0.65	0.07	0.16	0.03	0.14	0.28	0.23	1.86
	Average	19.64	3.22	2.51	1.06	2.41	13.67	2.03	61.54

when compared to glacierized catchments. Overall, Na^+ and Cl^- concentrations do not show any observable trend with glacier coverage. With the exception of Mg^{2+} and SO_4^{2-} GoA concentrations of the major ions and SiO_2 are elevated in glacier fed rivers compared to the global glacier river compilation from Torres et al. (2017).

4.2. Major Element Fluxes

The total elemental fluxes (uncorrected for rain) are detailed in Table 3 and indicate regional differences in the variability of fluxes across the GoA. Average fluxes of the major ions and SiO_2 are highest in the CR and CC regions. The watersheds of the SR and SE regions follow with the second highest average fluxes. Of the seven regions, the WCI has the lowest average fluxes, while the KP and PWS have the fifth and sixth highest average fluxes. In general, watersheds with high and medium glacier coverage had the greatest average flux values across

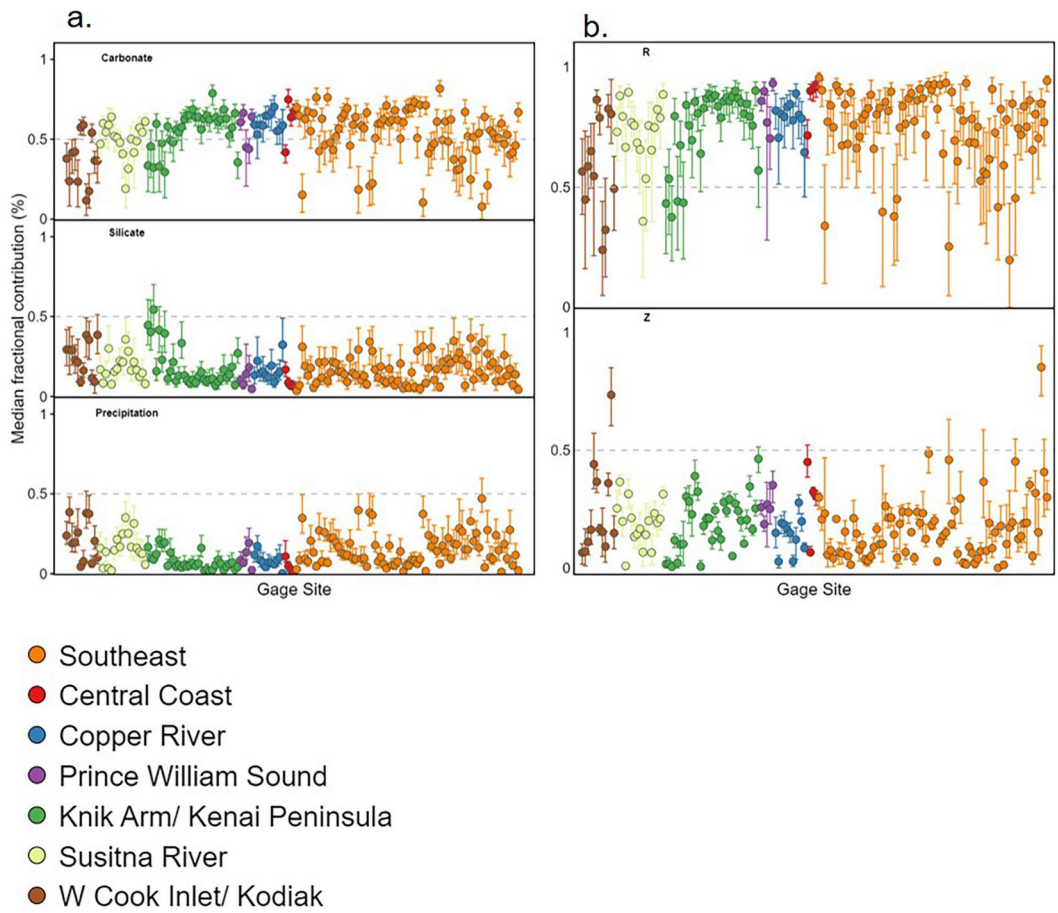

Figure 3. Median fractional contributions from each endmember that contributes cations (a) and the median *R* and *Z* parameters for each stream (b). Stream sites are arranged by longitude and from left to right on the *x*-axis correspond to a west to east transect across the Gulf of Alaska. Error bars represent the 25th and 75th percentiles.

the GoA. An exception is the SE region, where low glacier cover watersheds have the highest fluxes regionally. Element fluxes in the non-glacierized watersheds are much less compared with those in the glacierized basins.

All cation fluxes are elevated in the glacierized watershed compared with the non-glacierized. Across all regions Ca^{2+} has the highest flux of the cations followed by either Mg^{2+}, in the case of SE and CC, and Na^{+} in all other regions. Average SiO_2 fluxes are primarily the greatest in high and medium glacier coverage watersheds; however, in the SE, the low glacier coverage watersheds are the most elevated. Bicarbonate fluxes are the highest followed by SO_4^{2-}; both being elevated in glacierized watersheds.

4.3. Inversion Results

4.3.1. Endmember Contributions

Figure 3a shows the median fractional contributions from carbonate, silicate, and precipitation for each stream site with uncertainty represented by error bars at the 25th and 75th percentiles. The fractional contribution of carbonate is generally higher compared to the other endmembers. The MEANDIR inversion computations, resulted in a median fractional contribution with the 25th and 75th in parentheses, when aggregated across all GoA sample sites, of 55 (42–64)% from carbonate, with the silicate, and precipitation end-members contributing 14 (8–25)% and 9 (4–19)%, respectively. Pyrite weathering, not reported in Figure 3, contributes only 13 (7–18)% of the solute load across the GoA. Recently, Pappala et al. (2023) calculated weathering fractions associated with the Matanuska River located within the KP region. They calculated that atmospheric inputs (precipitation) to the Matanuska River to be roughly 5% of the total dissolved load, while our model estimates an average of 6% of the

dissolve load from precipitation at the Matanuska River (USGS site 15284000). Additionally, we estimate that silicate weathering fraction to be 13% and Pappala et al. (2023) estimate an average of 14%. This gives an indication that the overall results of our broad modeling effort produce reasonable results.

Calcium is primarily sourced from the carbonate endmember with a median contribution of 79 (64–90)%. The carbonate and silicate end-members are both important sources of Mg^{2+} contributing 64 (36–83)% and 21 (7–46)% respectively. In our model, we allow Na^+ to be sourced from silicate and precipitation only. The silicate endmember supplies 77 (54–91)% of Na^+, whereas precipitation contributes 20 (8–44)%. Sulfate is primarily sourced from pyrite weathering or precipitation; however, we do allow a very minor contribution from the carbonate endmember, though the fractional contribution in this case is less than one percent. Overall pyrite provides 84 (60–94)% and precipitation contributes 14 (5–39)% of the SO_4^{2-} to the rivers of the GoA.

4.3.2. *R* and *Z* Parameters

Across all samples in our dataset, carbonates (R) account for a median fractional contribution of 78 (63–88)% of the cations sourced from chemical weathering. The fractional contribution of the silicate endmember from chemical weathering to cation flux is equivalent to $1 - R$. The median value for the weathering done by H_2SO_4, the parameter Z, across all GoA watersheds is 19 (9–27)%. Figure 3b illustrates the variability in the R and Z values for each stream site. Stream sites with lower R values within this dataset generally also have decreased Z values. We use the 25th and 75th percentiles with error bars to show the uncertainty of the model results.

4.3.3. Weathering Yields

Yield values for cations derived from the sum total of weathering from silicate and carbonate minerals along with SiO_2 are plotted against stream runoff in Figures 4a and 4b. Here we focus on the regions that provide the most data and observe that the KP and SR regions both have elevated cation weathering rates at similar runoff values compared to the SE regions. Additionally, in the SR and KP regions, there is limited overlap between the weathering yields in non-glacierized and glacierized watersheds, while in the SE region, many of the non-glacier fed streams have similar weathering rates as the glacier fed streams. Yields of SiO_2 across the SR, KP and SE show considerable variability (Figure 4b). In the KP region, there are several watersheds that have equal or higher SiO_2 yields at lower runoff than most of the other streams. In the SE region, the glacierized and non-glacierized watersheds have similar SiO_2 yields, while there is separation between the glacierized and non-glacierized SiO_2 yields.

Compared to a global river data set (Gaillardet et al., 1999), cation yields derived from silicate weathering are generally lower (Figure S3a in Supporting Information S1). However, there is overlap between the GoA and global river values at lower runoff. Interestingly, the yields from the GoA streams are elevated compared to the global high-latitude rivers. The global high-latitude rivers are a subset of the Gaillardet et al. (1999) dataset that includes the Mackenzie, Ob, Yukon, and Kuskokwim Rivers. Except for several non-glacierized streams in the KP region, SiO_2 yields are also lower in GoA rivers compared to the global dataset (Figure S3b in Supporting Information S1). We also compare total cation weathering rates and SiO_2 yields of GoA streams against a global dataset of glacier fed streams (Torres et al., 2017). GoA rivers have similar cation weathering rates as the global glacier rivers (Figure S3c in Supporting Information S1). In terms of SiO_2, many GoA streams have greater yields compared to the global glacier rivers (Figure S3d in Supporting Information S1).

5. Discussion

5.1. Weathering Reactions

Our weathering investigation focuses on attributing cation and SO_4^{2-} to the prescribed endmembers, and with post inversion calculations we can infer the fraction of weathering done by sulfuric acid or by CO_2. In our study setup, the possible weathering reactions are silicate and carbonate dissolution by carbonic acid or silicate and carbonate dissolution by sulfuric acid. Due to the extremely minor occurrences of evaporites, we assume that evaporite weathering provides an extremely low contribution to the overall stream chemistry throughout the GoA. Each reaction generates a unique ratio of the cations and anions involved. Figures 5a and 5b are graphical representations of chemical weathering of silicates by carbonic or sulfuric acid (Equation S7 in Supporting Information S1). Similarly Figures 5c and 5d show carbonate dissolution by sulfuric acid, respectively. For clarity, we

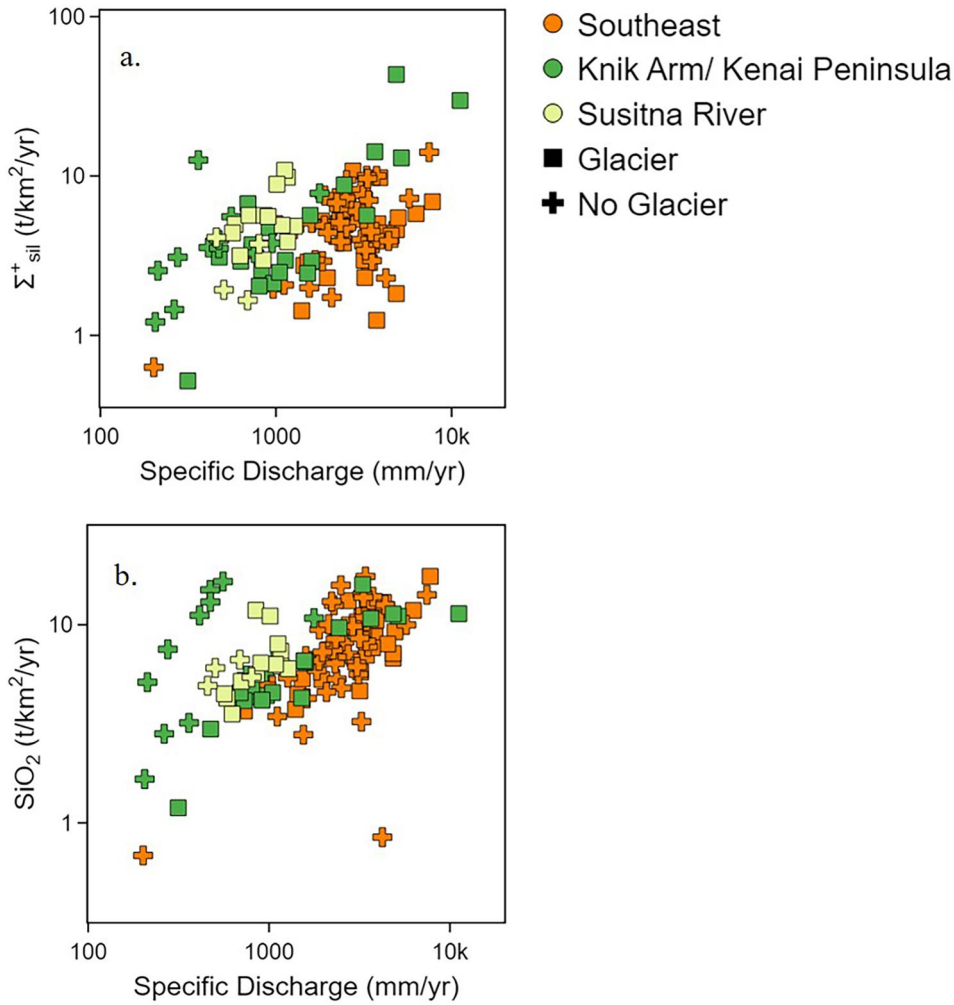

Figure 4. Cation yield derived from silicate weathering versus runoff (a) and SiO_2 yield versus runoff (b).

have removed two outliers from these plots in order to focus on the primary trends we observe (plots with the outliers can be found in Figure S4 in Supporting Information S1). Several details of the controls on stream water chemistry are apparent from Figure 5. First, glacier fed rivers have unique chemistry compared with non-glacier fed. Second, at the high end of the concentrations, glacier fed stream chemistry tends to plot nearer the line indicating weathering by sulfuric acid.

Furthermore, the two parameters *R* (fraction of cations from carbonates) and *Z* (fraction of weathering acid from FeS_2 oxidation) can be used to better understand the variability of weathering regimes in the GoA watersheds. Figure 6 shows the median values of each stream in *Z* versus *R* space. This framework and graphical visualization can be used to illustrate how weathering by sulfuric acid can, on geologic time scales, counteract the CO_2 drawdown that occurs through chemical weathering (Kemeny et al., 2021; Torres et al., 2016). This is done by examining the relationship between alkalinity and dissolved inorganic carbon (DIC), which are two important parameters moderating Earth's long-term carbon cycles. Within the framework of this study, our intention is primarily to show how the contribution of sulfuric acid weathering varies between glacier fed and non-glacier fed streams (Figure 6) and the regions across the GoA (see Figure S5 in Supporting Information S1). In addition to global carbon cycling, this has implications for the overall water quality of freshwater discharged to the GoA. We suggest that weathering driven by sulfuric acid within glacierized watersheds is likely one of the primary pathways driving the elevated cation concentrations we observe (Table 1, Figure 5). Additionally, the production of sulfuric acid by sulfide oxidation can act to alter the alkalinity budget within rivers, further adjusting water chemistry. Throughout the GoA, we observe the weathering generated by sulfuric acid to be elevated within

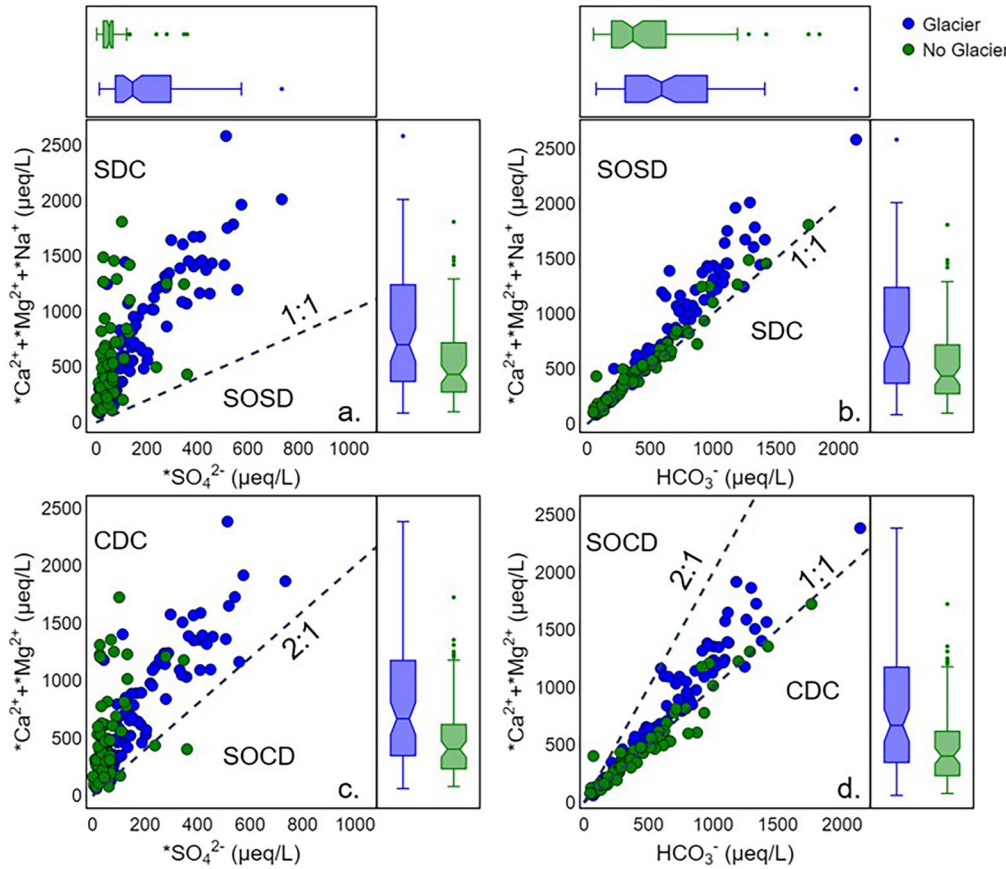

Figure 5. Weathering reactions, similar to Hindshaw et al. (2016). Each point represents the calculated mean value and the star (*) denotes the solute concentration that has been corrected for precipitation. Panels (a) and (b) show Gulf of Alaska (GoA) streams in a space to observe weathering of silicates by either carbonic acid or sulfuric acid. Silicate dissolution by carbonic acid (SDC) is greatest in non-glacierized watersheds, while glacierized basin plots are closer to the sulfide oxidation coupled silicate dissolution weathering pathway. Panels (c) and (d) show carbonate dissolution by carbonic acid (CDC) or sulfide oxidation coupled to carbonate dissolution (SOCD). Similarly, non-glacierized watershed plots are closer to the CDC region, whereas glacierized streams are closer to the SOCD region.

glacierized watersheds. There are two non-glacierized watersheds that we observe to have quite high calculated weathering by sulfuric acid. It is unclear from the geology what may cause this; therefore, we hypothesize that there may be either an unknown evaporite source or mineralization that occurs within the respective watersheds. Increased physical weathering within a watershed has been implicated in describing the mechanism that controls observed elevated weathering caused by sulfuric acid (Calmels et al., 2007; Kemeny et al., 2021; Torres et al., 2014, 2016). We infer that elevated physical erosion via glacier abrasion and frost cracking (Horan et al., 2017) provides fresh mineral surfaces that are readily weathered, leading to elevated weathering contributions from sulfuric acid. Additionally, in recently deglacierized areas, low vegetation coverage and soil development expose bedrock to the atmosphere, further leading to increases in oxidative weathering (Horan et al., 2017).

5.2. Watershed Controls on Weathering Regimes

Chemical weathering of carbonates is the primary source of solutes to streams in the GoA. However, there are several watersheds in which silicate weathering is an important contributor to the solute flux (Figure 7). Streams where silicate weathering is elevated are found in watersheds of the WCI, KP, and SR regions. These streams are in non-glacierized basins characterized by low elevation and relief with elevated mean annual air temperature. Specifically, within the southern KP region, these watersheds are distinctive within our datasets due to the fact that the streams and rivers are not fed by a mountain range and referred to as the Kenai Lowlands. Streams and

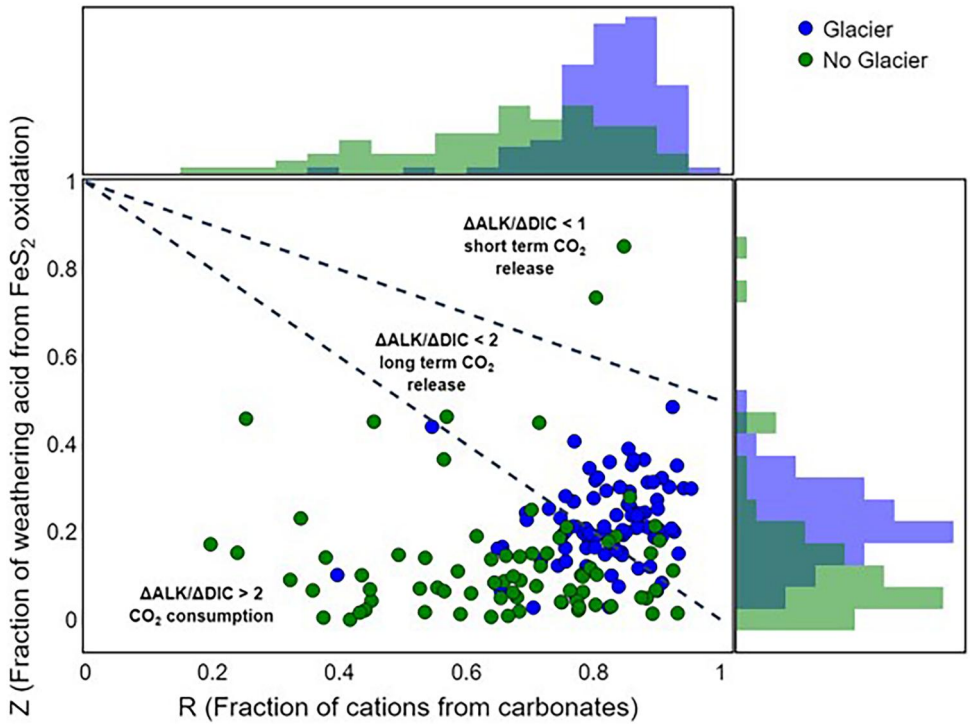

Figure 6. Similar to Torres et al. (2016), we show the median values of *Z* versus *R*. Although this plot is primarily suited to ascertain information concerning the short- and long-term C cycle, we use it to further illustrate how weathering done by sulfuric acid is generally greater within glacierized basins. Additionally, we observe that *R* values are more likely to be elevated within glacierized basins.

rivers in this area are fed by yearly snow and rain and numerous groundwater springs. This area is well studied by fish biologists and stream ecologists because it is a prime area for pacific salmon to spawn (King et al., 2012; Walker et al., 2021). It is believed that the groundwater sources provide some thermal buffering during the winter months and provide an excellent environment for salmon rearing (Callahan et al., 2015). As such, we hypothesize that because these streams and rivers likely have a large proportion of their water sourced from groundwater that this enhances silicate weathering. This is also observed in Figure 7 that maps the silicate fraction at each sample site by a cluster of red points in the mid-left of the plot. Because silicate weathering is dependent on temperature and the groundwater provides an environment in which water temperatures remain elevated, compared to glacierized streams or even alpine streams, silicate weathering is likely enhanced because of the increased temperatures.

Another area in the GoA where silicate weathering is an important source of solutes are streams in the SE region on the islands that make up the Alexander Archipelago. These watersheds are some of the smallest in the dataset, are non-glacierized, and receive a significant amount of precipitation as rain. The fractional contribution of cations from carbonate weathering, the *R* parameter, is positively related to glacier coverage ($r = 0.38$, $p \ll 0.05$). We also observe that the fraction of silicate weathering is negatively related to glacier coverage ($r = -0.4$, $p \ll 0.05$). Throughout the GoA, there are few watersheds in which silicate weathering is dominant based on solute production. Several physically based factors drive these relationships. Regardless of primary lithology, carbonate weathering controls the solute fluxes in glacierized basins (Tranter & Wadham, 2003). This is because silicate weathering is highly dependent on temperature and carbonate dissolution kinetics are 6–9 times faster than those of silicate minerals (Anderson, 2005, 2007). Even within the non-glacierized watersheds, the overall low air temperatures throughout the GoA can limit silicate weathering.

We observe silicate weathering to be positively related to watershed mean annual air temperature (Figure 8 and Table S3; $r = 0.33$, $p < 0.05$). Additionally, the fractional contribution of silicate weathering is negatively related to relief (Figure 8 and Table S3; $r = 0.39$, $p < 0.05$). Air temperatures within glacierized watersheds are lower compared to non-glacierized watersheds likely due to the elevation in which the watersheds exist. In addition to

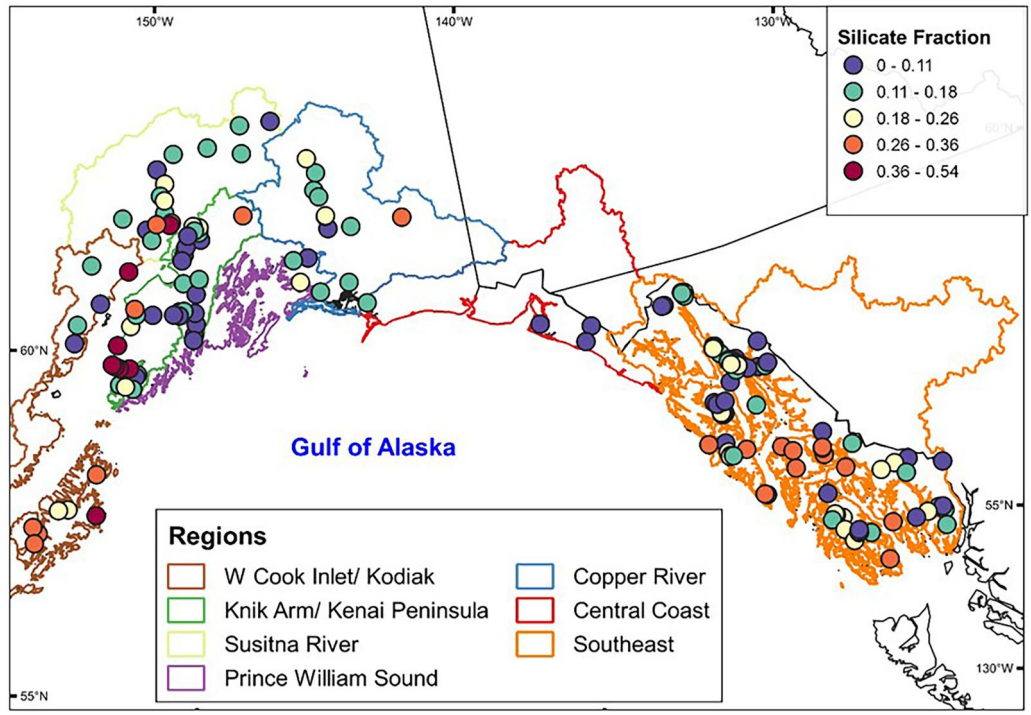

Figure 7. Median fractional contributions from silicate weathering for each stream site across the Gulf of Alaska. There are several streams in the southern portion of the Knik Arm/Kenai Peninsula (KP) region that have elevated silicate weathering. Additionally, within the Southeast (SE) region there are several sites where silicate weathering is an important contributor of solutes.

the decreased air temperature, Fellman, Nagorski, et al. (2014) showed that water temperature is negatively related to glacier coverage, which can lead to further lowering the rate of silicate weathering in the sub and proglacial zones (Anderson, 2005). With continued glacier recession and increasing air and river water temperatures, the fractional contribution from silicate weathering will likely increase in the future.

Carbonate weathering has a moderately positive relationship with elevation in our dataset. This is not to say that high elevation causes carbonate weathering to be enhanced, but rather that the mean elevation is correlated to many other watershed characteristics that can aid in explaining the variability in carbonate weathering within the dataset. Mean watershed elevation and mean temperature are strongly negatively related ($r = -0.82$, $p < 0.05$), while elevation is positively related to relief ($r = 0.73$, $p < 0.05$) and glacier coverage ($r = 0.54$, $p < 0.05$). The fraction of silicate weathering is diminished in these environments such that carbonate weathering dominates the solute load even if carbonates are found in trace amounts within a given watershed. Especially in watersheds of the GoA, due to the mixed lithology, changing glacier coverage and warming climate will feasibly cause the ratio between carbonate and silicate weathering to decrease. Through time, as weathering surfaces age and physical weathering decreases, silicate weathering will become a more important source of solutes (Jacobson et al., 2002). However, carbonate weathering will likely continue to be the dominant source of weathering products through the end of the century.

Glacier cover and relief drive regional and watershed to watershed variability of sulfuric acid weathering. Glacier coverage and relief are positively related, confounding the interpretation of what characteristics ultimately drive sulfide weathering. Z values in non-glacierized basins are positively related to relief, implying that relief by itself is a key watershed characteristic that may have strong controls on sulfide oxidation (Calmels et al., 2007; Torres et al., 2014). Both glacier coverage and watershed relief may be thought of as proxies for erosion. Sulfide weathering is supply limited indicating that environments prone to erosion may be conducive to sulfide weathering. The positive relationship between the Z parameter and relief (a proxy for erosion) across the GoA is shown in Figure 8. We observe in Figure 8 that there is a negative correlation between the primary lithology types in the GoA and Z values, while other watershed characteristics such as glacier coverage, relief, elevation and

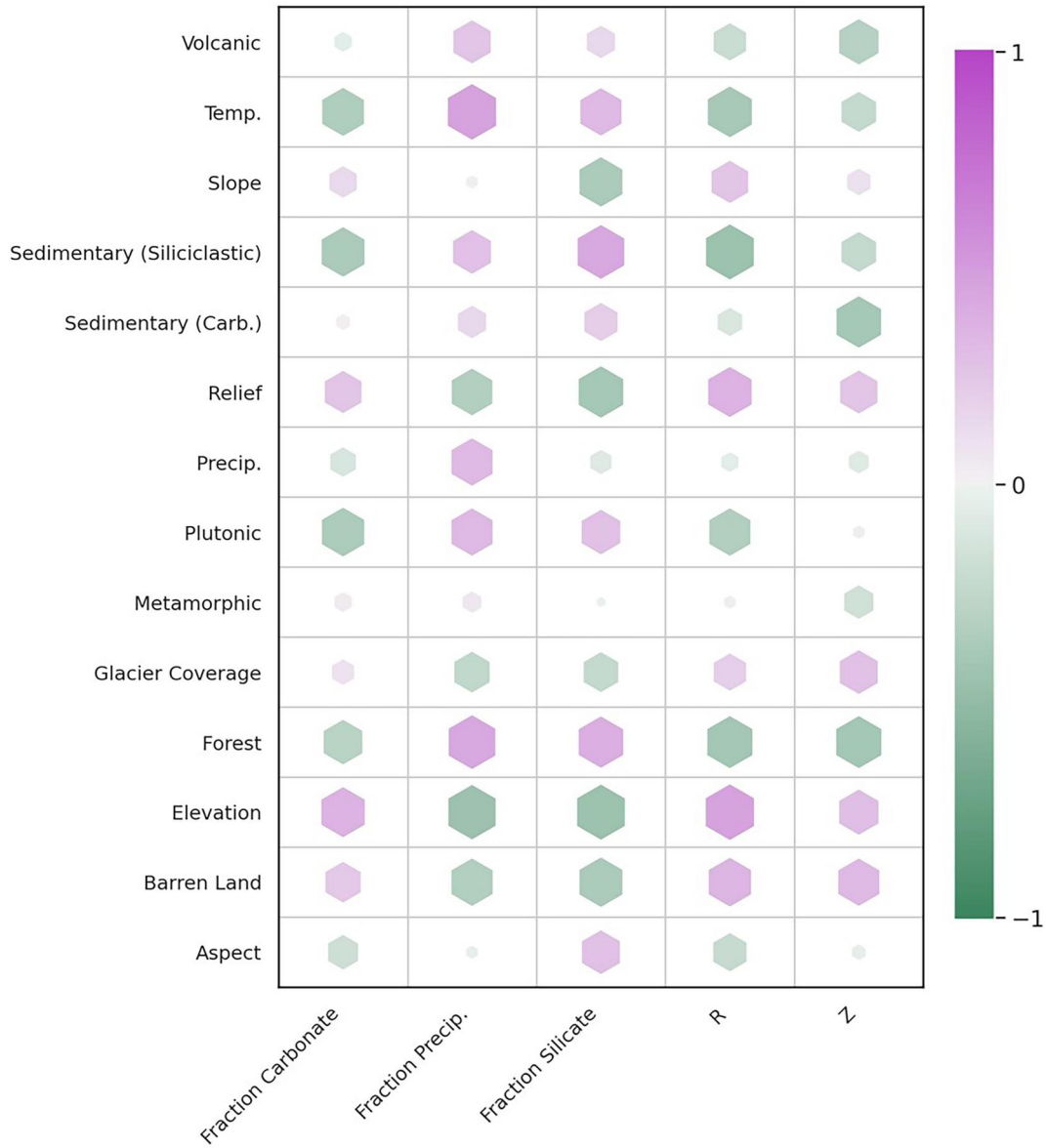

Figure 8. Heatmap illustrating the calculated Pearson's *r* value for the correlations between the calculated fractional contributions of end-members and the *R* and *Z* values. The size of the hexagon relates to the magnitude of the *r* value.

barren land are positively related. This indicates that topography and land cover are some of the primary controls on elevating weathering by sulfuric acid in the GoA. Ultimately, in our dataset and model results, watershed lithology acts as a secondary control to the geomorphology and topography in terms of weathering driven by sulfide oxidation. Except for a few outliers, median values for the fraction of weathering by sulfuric acid are capped below 0.4. This is likely from the secondary effects of lithology or the dependence of sulfide oxidation on seasonal runoff patterns (Kemeny et al., 2021; Winnick et al., 2017). Overall, sulfide weathering is an important driver of stream chemistry within the GoA region and changes in landcover and glacier coverage may affect the relative proportion of solutes derived from chemical weathering coupled to sulfide weathering.

5.3. Regional and Global Perspective on Weathering Yields

Throughout the GoA, total fluxes (non-area weighted) of the major cations and SiO_2 are generally elevated in glacierized basins (Table 3). This highlights the importance of glacierized basins in exporting solutes and major and minor nutrients to the nearshore environment. However, it is important to view the results of our weathering

model in terms of area weighted flux, or yields. Often within watersheds, especially glacierized watersheds, a relatively small area of the basin may be responsible for supplying most of the flux of solutes. Weighting flux by area is preferable when illustrating a watersheds overall efficiency in transporting solutes and freshwater.

The yields of chemical weathering products drive river water quality and deliver vital solutes and nutrients to nearshore ecosystems (Huss et al., 2017; Milner et al., 2017). Shifting climate regimes and glacier recession will result in changes in river runoff, which is a primary driver of weathering yields. Previous work by Jenckes et al. (2023) hypothesized that if all glaciers within the GoA were to melt, cation yields would diminish. However, this does not consider the predicted increase in precipitation. We observe elevated precipitation in the SE region and weathering derived yields are very similar in non-glacierized and glacierized watersheds. Currently, the non-glacierized basins in the SE are relatively small catchments that receive some of the highest amounts of precipitation in the GoA. Therefore, within the SE weathering rates in glacierized and non-glacierized watersheds can be similar because of elevated specific discharge. Thus, implying that elevated precipitation may result in similar weathering yield despite glacier loss. Contrastingly, we found that weathering yields in non-glacierized regions in the KP and SR regions are lower compared to glacierized basins. In these two regions, the glacier coverage has a stronger control on runoff due to the lower amounts of precipitation in Southcentral Alaska. Jenckes et al. (2023) and separately Bergstrom et al. (2021) illustrated that climate (precipitation as rain) ultimately controls seasonal solute yields. The studied watersheds in KP and SR, both non-glacierized and glacierized, are much larger compared to most SE watersheds, which will likely lead to a different response in terms of weathering yields and runoff to increased precipitation as rain (Andermann et al., 2012; Asano et al., 2020).

We observe that yields from silicate weathering and yields of SiO_2 are generally lower at similar runoff in the GoA streams compared to the global rivers (Figures S3c and S3d in Supporting Information S1). This is despite watersheds in the GoA containing high areal coverage of plutonic, volcanic, and siliciclastic sediment lithologies that would suggest higher amounts of weathering yields derived from silicate weathering. Overall cooler air and water temperatures within the GoA region provide the most plausible explanation for this observation. On the other hand, compared to the global glacier dataset, GoA watersheds are similar in terms of chemical weathering rates and yields of SiO_2 (Figure S3d in Supporting Information S1). Additionally, in the GoA dataset, there are several stream sites that have runoff values that exceed what has been compiled in both global compilation datasets. Such extremes are important for identifying "hotspots" of weathering fluxes (e.g., Andrews et al., 2011).

5.4. Future Implications

Future changes to glacier coverage, temperature, and precipitation regimes will alter nutrient and solute fluxes to the GoA by modifying freshwater runoff and chemical weathering regimes. There are three primary changes to weathering regimes that we hypothesize will occur by the end of the century due to shifting climate. First, silicate weathering will increase relative to carbonate weathering. This is driven not only by increased air and water temperature but also by an increase in proglacial area, which previously has been indicated to increase silicate weathering (Anderson, 2005). Second, loss of glacier ice coverage will lower rates of sulfuric acid driven chemical weathering due to decreased mineral supply caused by decreases in the rates of erosion driven by glaciers. Other physical weathering dynamics can supply fresh mineral surfaces once glacier coverage diminishes, such as frost cracking and landslides. Finally, in regions of Southcentral Alaska (i.e., SR and KP regions), glacier ice loss will result in diminished yields of weathering derived solutes, however, the predicted increase in precipitation will likely offset some of the loss in yields by keeping stream runoff elevated (Beamer et al., 2017). The increase in precipitation will affect weathering yields and runoff in the smaller coastal catchments compared to the larger inland basins that are situated in the KP, SR, and CR regions. The interpretation of the changes in water chemistry based on altered future landscape and precipitation patterns is based on climate scenarios forecasted to the end of the century. As such, we expect that changes to chemical weathering patterns will adjust variably across the GoA as different amounts of glacier coverage currently exist.

These hypothesized changes in weathering regimes have implications for overall stream chemistry and solute yields. Increased silicate weathering may increase concentrations of Na^+, Mg^{2+}, and SiO_2, lowering the relative dominance of Ca^{2+}. Importantly, SiO_2 flux from rivers to the nearshore ecosystem is an important nutrient for primary producers. In the KP and SR regions, solute yields derived from weathering will likely decrease as glacier coverage declines. Changing cation, anion, and SiO_2 concentrations and rising water temperatures will directly affect water quality, which can alter both in stream and nearshore coastal and estuarine ecosystems (Huss

et al., 2017; Milner et al., 2017). However, there is limited work, especially in the GoA region, establishing the extent to which ecosystems will be affected. Lower sulfide oxidation coupled to carbonate dissolution will likely lead to an increase in the ratio of alkalinity to DIC delivered to the GoA (Torres et al., 2017). This change would be driven by an increase in the ratio of weathering by carbonic acid compared to sulfuric acid. These ratios have important implications for ocean acidification modeling efforts within the GoA (Hauri et al., 2020), which rely on a spatially limited dataset of coastal freshwater quality for model forcing. Further investigation is required to understand how the modifications of alkalinity and DIC will be altered as stream runoff dynamics change under future climate regimes.

6. Conclusions

To investigate chemical weathering regimes across the GoA, we applied an inversion model, MEANDIR, to a large dataset of river water chemistry derived from the USGS NWIS and a novel set of stream sites (Jenckes et al., 2023). We found that carbonate weathering dominates the solute flux of chemical weathering derived products. However, there are several watersheds in the WCI, KP and SE regions in which silicate weathering is elevated compared to most other watersheds. Within glacierized basins, weathering by sulfuric acid is elevated compared with non-glacierized catchments. Compared to the world's largest rivers, cation yields from silicate weathering and SiO_2 yields are generally lower within GoA watersheds. Alternatively, GoA streams have similar total cation weathering rates and SiO_2 yields to a global compilation of glacier fed rivers. With the results of the weathering model, we hypothesize that as rain amounts increase, watersheds lose glacier ice, and as temperatures rise, the weathering regimes will adjust such that (a) the fractional contribution from silicate weathering will increase, (b) weathering promoted by sulfuric acid will decrease, and (c) weathering rates in Southcentral Alaska will likely decline due to decreased glacier coverage. The work presented here is the first to apply an inverse weathering model, investigate the role of sulfide oxidation, and put weathering rates of GoA streams within a global context. Further work is needed to link the effects of changes in fluxes of chemical weathering derived products on downstream ecosystems.

Data Availability Statement

Data derived from the USGS database can be downloaded through the USGS NWIS at https://waterdata.usgs.gov/nwis. Data derived from Jenckes et al. (2023) are located at http://hdl.handle.net/11122/13099. All other data used in the manuscript can be found in Supporting Information S1.

Acknowledgments
We would like to thank Bob Hilton and two anonymous reviewers for feedback that improved the quality of this manuscript. Funding for this research was provided by National Science Foundation (NSF) award OIA-1757347 to Lee Ann Munk and others. Jordan Jenckes received support from the Sloan Indigenous Graduate Partnership Fellowship and the Aleut Foundation Graduate Scholarship program. Sebastian Muñoz acknowledges support from the NSF Graduate Research Fellowships Program (GRFP), The Brown University Presidential Fellowship, and the Institute at Brown for Environment and Society (IBES) Graduate Research Travel & Training Grant.

References

Andermann, C., Longuevergne, L., Bonnet, S., Crave, A., Davy, P., & Gloaguen, R. (2012). Impact of transient groundwater storage on the discharge of Himalayan rivers. *Nature Geoscience*, *5*(2), 127–132. https://doi.org/10.1038/ngeo1356

Anderson, S. P. (2005). Glaciers show direct linkage between erosion rate and chemical weathering fluxes. *Geomorphology*, *67*(1–2 SPEC. ISS), 147–157. https://doi.org/10.1016/j.geomorph.2004.07.010

Anderson, S. P. (2007). Biogeochemistry of glacial landscape systems. https://doi.org/10.1146/annurev.earth.35.031306.140033

Anderson, S. P., Drever, J. I., & Humphrey, N. F. (1997). Chemical weathering in glacial environments. *Geology*, *25*(5), 399–402. https://doi.org/10.1130/0091-7613(1997)025<0399:CWIGE>2.3.CO

Andrews, D. M., Lin, H., Zhu, Q., Jin, L., & Brantley, S. L. (2011). Hot spots and hot moments of dissolved organic carbon export and soil organic carbon storage in the Shale Hills catchment. *Vadose Zone Journal*, *10*(3), 943–954. https://doi.org/10.2136/vzj2010.0149

Armstrong, A. K., & MacKevett, E. M., Jr. (1977). *The Triassic Chitisone Limestone, Wrangall Mountains, Alaska—Stressing detailed descriptions of sabkha facies and other rocks in lower parts of the Chitisone and their relations to Kennecott-type copper deposits*. Report 77-217. U.S. Geological Survey. Retrieved from https://pubs.usgs.gov/publication/ofr77217

Asano, Y., Kawasaki, M., Saito, T., Haraguchi, R., Takatoku, K., Saiki, M., & Kimura, K. (2020). An increase in specific discharge with catchment area implies that bedrock infiltration feeds large rather than small mountain headwater streams. *Water Resources Research*, *56*(9), e2019WR025658. https://doi.org/10.1029/2019WR025658

Beamer, J. P., Hill, D. F., Arendt, A., & Liston, G. E. (2016). High-resolution modeling of coastal freshwater discharge and glacier mass balance in the Gulf of Alaska watershed. *Water Resources Research*, *52*(5), 3888–3909. https://doi.org/10.1002/2015WR018457

Beamer, J. P., Hill, D. F., McGrath, D., Arendt, A., & Kienholz, C. (2017). Hydrologic impacts of changes in climate and glacier extent in the Gulf of Alaska watershed. *Water Resources Research*, *53*(9), 7502–7520. https://doi.org/10.1002/2016WR020033

Bergstrom, A., Koch, J. C., O'Neel, S., & Baker, E. (2021). Seasonality of solute flux and water source chemistry in a coastal glacierized watershed undergoing rapid change: Wolverine glacier watershed, Alaska. *Water Resources Research*, *57*(11), e2020WR028725. https://doi.org/10.1029/2020WR028725

Bradley, D. C., Kusky, T. M., Haeussler, P. J., Karl, S. M., & Donley, D. T. (1999). Geologic map of the Seldovia quadrangle, south-central Alaska. U.S. Geological Survey Open-File Report OFR 99-18G.

Brennan, S. R., Fernandez, D. P., Mackey, G., Cerling, T. E., Bataille, C. P., Bowen, G. J., & Wooller, M. J. (2014). Strontium isotope variation and carbonate versus silicate weathering in rivers from across Alaska: Implications for provenance studies. *Chemical Geology*, *389*, 167–181. https://doi.org/10.1016/j.chemgeo.2014.08.018

Burke, A., Present, T. M., Paris, G., Rae, E. C. M., Sandilands, B. H., Gaillardet, J., et al. (2018). Sulfur isotopes in rivers: Insights into global weathering budgets, pyrite oxidation, and the modern sulfur cycle. *Earth and Planetary Science Letters*, *496*, 168–177. https://doi.org/10.1016/j.epsl.2018.05.022

Callahan, M. K., Rains, M. C., Bellino, J. C., Walker, C. M., Baird, S. J., Whigham, D. F., & King, R. S. (2015). Controls of temperature in salmonid-bearing headwater streams in two common hydrogeologic settings, Kenai Peninsula, Alaska. *Journal of the American Water Resources Association (JAWRA)*, *51*(1), 84–98. https://doi.org/10.1111/jawr.12235

Calmels, D., Gaillardet, J., Brenot, A., & France-Lanord, C. (2007). Sustained sulfide oxidation by physical erosion processes in the Mackenzie River basin: Climatic perspectives. *Geology*, *35*(11), 1003–1006. https://doi.org/10.1130/G24132A.1

CCRS. (2015). 2015 Land cover of North America at 30 meters. Retrieved from http://www.cec.org/nalcms

Colbourn, G., Ridgwell, A., & Lenton, T. M. (2015). The time scale of the silicate weathering negative feedback on atmospheric CO_2. *Global Biogeochemical Cycles*, *29*(5), 583–596. https://doi.org/10.1002/2014GB005054

Cole, T. L., Torres, M. A., & Kemeny, P. C. (2022). The hydrochemical signature of incongruent weathering in Iceland. *Journal of Geophysical Research: Earth Surface*, *127*(6), e2021JF006450. https://doi.org/10.1029/2021JF006450

Curran, J. H., & Biles, F. E. (2021). Identification of seasonal streamflow regimes and streamflow drivers for daily and peak flows in Alaska. *Water Resources Research*, *57*(2), e2020WR028425. https://doi.org/10.1029/2020WR028425

Eckhart, R. A. (1951). Gypsiferous deposits on sheep mountain, Alaska. *Geology of Denmark Survey Bulletin*, *989*, 39–61.

Fellman, J. B., Hood, E., Spencer, R. G. M., Stubbins, A., Raymond, A., Fellman, J. B., et al. (2014). Watershed glacier coverage influences dissolved organic matter biogeochemistry in coastal watersheds of southeast Alaska. *Ecosystems*, *17*(6), 1014–1025. https://doi.org/10.1007/s10021-014-9777-1

Fellman, J. B., Nagorski, S., Pyare, S., Vermilyea, A. W., Scott, D., & Hood, E. (2014). Stream temperature response to variable glacier coverage in coastal watersheds of Southeast Alaska. *Hydrological Processes*, *28*(4), 2062–2073. https://doi.org/10.1002/hyp.9742

Gaillardet, J., Dupre, B., Louvat, P., & Allegre, C. J. (1999). Global silicate weathering and CO_2 consumption rates deduced from the chemistry of large rivers. *Chemical Geology*, *159*(1–4), 3–30. https://doi.org/10.1016/s0009-2541(99)00031-5

Garrels, R. M., & Mackenzie, F. T. (1967). Origin of the chemical compositions of some springs and lakes. In *Equilibrium concepts in natural water systems* (pp. 222–242).

Hartmann, J., & Moosdorf, N. (2012). The new global lithological map database GLiM: A representation of rock properties at the Earth surface. *Geochemistry, Geophysics, Geosystems*, *13*(12), Q12004. https://doi.org/10.1029/2012GC004370

Hauri, C., Schultz, C., Hedstrom, K., Danielson, S., Irving, B., Doney, S. C., et al. (2020). A regional hindcast model simulating ecosystem dynamics, inorganic carbon chemistry, and ocean acidification in the Gulf of Alaska. *Biogeosciences*, *17*(14), 3837–3857. https://doi.org/10.5194/BG-17-3837-2020

Hindshaw, R. S., Heaton, T. H. E., Boyd, E. S., Lindsay, M. R., & Tipper, E. T. (2016). Influence of glaciation on mechanisms of mineral weathering in two high Arctic catchments. *Chemical Geology*, *420*, 37–50. https://doi.org/10.1016/j.chemgeo.2015.11.004

Hood, E., & Berner, L. (2009). Effects of changing glacial coverage on the physical and biogeochemical properties of coastal streams in southeastern Alaska. *Journal of Geophysical Research*, *114*(G3), 3001. https://doi.org/10.1029/2009JG000971

Hood, E., Fellman, J. B., & Spencer, R. G. M. (2020). Glacier loss impacts riverine organic carbon transport to the ocean. *Geophysical Research Letters*, *47*(19), 1–9. https://doi.org/10.1029/2020GL089804

Horan, K., Hilton, R. G., Selby, D., Ottley, C. J., Gröcke, D. R., Hicks, M., & Burton, K. W. (2017). Mountain glaciation drives rapid oxidation of rock-bound organic carbon. *Science Advances*, *3*(10), e1701107. https://doi.org/10.1126/sciadv.1701107

Huss, M., Bookhagen, B., Huggel, C., Jacobsen, D., Bradley, R. S., Clague, J. J., et al. (2017). Toward mountains without permanent snow and ice. *Earth's Future*, *5*, 418–435. https://doi.org/10.1002/2016EF000514

IPCC. (2022). In H.-O. Pörtner, D. C. Roberts, M. Tignor, E. S. Poloczanska, K. Mintenbeck, et al. (Eds.), *Climate change 2022: Impacts, adaptation, and vulnerability. Contribution of Working Group II to the sixth assessment report of the Intergovernmental Panel on Climate Change* (p. 3056). Cambridge University Press. https://doi.org/10.1017/9781009325844

Jacobson, A. D., Blum, J. D., Chamberlain, C. P., Poage, M. A., & Sloan, V. F. (2002). Ca/Sr and Sr isotope systemics of a Himalayan glacial chronosequence: Carbonate versus silicate weathering rates a function of landscape surface age. *Geochemica et Cosmochimica Acta*, *66*(1), 13–27. https://doi.org/10.1016/S0016-7037(01)00755-4

Jenckes, J., Ibarra, D. E., & Munk, L. A. (2022). Concentration-discharge patterns adcross the Gulf of Alaska reveal geomorphological and glacierization controls on stream water solute generation and export. *Geophysical Research Letters*, *49*(1), e2021GL095152. https://doi.org/10.1029/2021GL095152

Jenckes, J., Munk, L. A., Ibarra, D. E., Boutt, D. F., Fellman, J., & Hood, E. (2023). Hydroclimate drives seasonal riverine export across a gradient of glacierized high-latitude coastal catchments. *Water Resources Research*, *59*(4), e2022WR033305. https://doi.org/10.1029/2022WR033305

Johnson, A. C., Bellmore, J. R., Haught, S., & Medel, R. (2019). Quantifying the monetary value of Alaska national forests to commercial Pacific salmon fisheries. *North American Journal of Fisheries Management*, *39*(6), 1119–1131. https://doi.org/10.1002/nafm.10364

Kang, M., Skierszkan, E., Brennan, S., Fernandez, D. P., Yang, Z., Girard, I., et al. (2022). Controls of lithium isotope spatial variability across the Yukon River: Implications for weathering processes in a warming subarctic basin. *Geochimica et Cosmochimica Acta*, *323*, 1–19. https://doi.org/10.1016/j.gca.2022.02.016

Kemeny, P. C., Lopez, G. I., Dalleska, N. F., Torres, M., Burke, A., Bhatt, M. P., et al. (2021). Sulfate sulfur isotopes and major ion chemistry reveal that pyrite oxidation counteracts CO_2 drawdown from silicate weathering in the Langtang-Trisuli-Narayani River system, Nepal Himalaya. *Geochimica et Cosmochimica Acta*, *294*, 43–69. https://doi.org/10.1016/J.GCA.2020.11.009

Kemeny, P. C., & Torres, M. A. (2021). Presentation and applications of mixing elements and dissolved isotopes in rivers (MEANDIR), a customizable MATLAB model for Monte Carlo inversion of dissolved river chemistry. *American Journal of Science*, *321*(5), 579–642. https://doi.org/10.2475/05.2021.03

King, R. S., Walker, C. M., Whigham, D. F., Baird, S. J., & Back, J. A. (2012). Catchment topography and wetland geomorphology drive macroinvertebrate community structure and juvenile salmonid distributions in south-central Alaska headwater streams. *Freshwater Science*, *31*(2), 341–364. https://doi.org/10.1899/11-109.1

Kusky, T. M., & Bradley, D. C. (1999). Kinematic analysis of mélange fabrics: Examples and applications from the McHugh Complex, Kenai Peninsula, Alaska. *Journal of Structural Geology*, *21*(12), 1773–1796. https://doi.org/10.1016/S0191-8141(99)00105-4

Lindsay, J. B. (2016). Whitebox GAT: A case study in geomorphometric analysis. *Computers & Geosciences*, *95*, 75–84. https://doi.org/10.1016/j.cageo.2016.07.003

Meybeck, M. (1987). Global chemical weathering of surficial rocks estimated from river dissolved loads. *American Journal of Science*, *287*(5), 401–428. https://doi.org/10.2475/ajs.287.5.401

Milner, A. M., Khamis, K., Battin, T. J., Brittain, J. E., Barrand, N. E., Füreder, L., et al. (2017). Glacier shrinkage driving global changes in downstream systems. *Proceedings of the National Academy of Sciences*, *114*(37), 9770–9778. https://doi.org/10.1073/pnas.1619807114

Moon, S., Chamberlain, C. P., & Hilley, G. E. (2014). New estimates of silicate weathering rates and their uncertainties in global rivers. *Geochimica et Cosmochimica Acta*, *134*, 257–274. https://doi.org/10.1016/j.gca.2014.02.033

Muñoz, S., Jenckes, J., Ramos, E. J., Munk, L. A., & Ibarra, D. E. (2024). Hydrologic and landscape controls on rock weathering along a glacial gradient in South Central Alaska, USA. *Journal of Geophysical Research: Earth Surface*, *129*, e2023JF007255. https://doi.org/10.1029/2023JF007255

Neal, E. G., Hood, E., & Smikrud, K. (2010). Contribution of glacier runoff to freshwater discharge into the Gulf of Alaska. *Geophysical Research Letters*, *37*(6), 1–6. https://doi.org/10.1029/2010GL042385

Négrel, P., Allegre, C. J., Dupré, B., & Lewin, E. (1993). Erosion sources determined by inversion of major and trace element ratios and strontium isotopic ratios in river water: The Congo Basin case. *Earth and Planetary Science Letters*, *120*(1–2), 59–76. https://doi.org/10.1016/0012-821x(93)90023-3

Pappala, V. S., Arendt, C. A., & Harmon, R. S. (2023). Spatial characterization of chemical weathering in a proglacial river system, southcentral Alaska. *Chemical Geology*, *629*, 121462. https://doi.org/10.1016/j.chemgeo.2023.121462

Quay, P. D., Wilbur, D. O., Richey, J. E., Devol, A. H., Benner, R., & Forsberg, B. R. (1995). The ^{18}O:^{16}O of dissolved oxygen in rivers and lakes in the Amazon Basin: Determining the ratio of respiration to photosynthesis rates in freshwaters. *Limnology and Oceanography*, *40*(4), 718–729. https://doi.org/10.4319/lo.1995.40.4.0718

Raiswell, R. (1984). Chemical models of solute acquisition in glacial melt waters. *Journal of Glaciology*, *30*(104), 49–57. https://doi.org/10.1017/S0022143000008480

Raymond, P. A., Hartmann, J., Lauerwald, R., Sobek, S., McDonald, C., Hoover, M., et al. (2013). Global carbon dioxide emissions from inland waters. *Nature*, *503*(7476), 355–359. https://doi.org/10.1038/nature12760

RGI Consortium. (2017). *Randolph Glacier Inventory—A dataset of global glacier outlines: Version 6.0*. Technical Report, Global Land Ice Measurements from Space. Digital Media. https://doi.org/10.7265/N5-RGI-60

Schoen, E. R., Wipfli, M. S., Trammell, E. J., Rinella, D. J., Floyd, A. L., Grunblatt, J., et al. (2017). Future of Pacific salmon in the face of environmental change: Lessons from one of the world's remaining productive salmon regions. *Fisheries*, *42*(10), 538–553. https://doi.org/10.1080/03632415.2017.1374251

Sergeant, C. J., Falke, J. A., Bellmore, R. A., Bellmore, J. R., & Crumley, R. L. (2020). A classification of streamflow patterns across the coastal Gulf of Alaska. *Water Resources Research*, *56*(2), 1–17. https://doi.org/10.1029/2019WR026127

Tadono, T., Ishida, H., Oda, F., Naito, S., Minakawa, K., & Iwamoto, H. (2014). Precise global DEM generation by ALOS prism. In *ISPRS annals of the photogrammetry, remote sensing and spatial information sciences, ISPRS Technical Commission IV Symposium, Suzhou, China* (Vol. II-4). https://doi.org/10.5194/isprsannals-II-4-71-2014

Thornton, M. M., Shrestha, R., Wei, Y., Thornton, P. E., Kao, S., & Wilson, B. E. (2020). *Daymet: Daily surface weather data on a 1-km grid for North America, Version 4*. ORNL DAAC. https://doi.org/10.3334/ORNLDAAC/1840

Torres, M. A., Moosdorf, N., Hartmann, J., Adkins, J. F., & West, A. J. (2017). Glacial weathering, sulfide oxidation, and global carbon cycle feedbacks. *Proceedings of the National Academy of Sciences of the United States of America*, *114*(33), 8716–8721. https://doi.org/10.1073/pnas.1702953114

Torres, M. A., West, A. J., Clark, K. E., Paris, G., Bouchez, J., Ponton, C., et al. (2016). The acid and alkalinity budgets of weathering in the Andes–Amazon system: Insights into the erosional control of global biogeochemical cycles. *Earth and Planetary Science Letters*, *450*, 381–391. https://doi.org/10.1016/j.epsl.2016.06.012

Torres, M. A., West, A. J., & Li, G. (2014). Sulphide oxidation and carbonate dissolution as a source of CO_2 over geological timescales. *Nature*, *507*(7492), 346–349. PMID: 24646998. https://doi.org/10.1038/nature13030

Tranter, M., Huybrechts, P., Munhoven, G., Sharp, M. J., Brown, G. H., Jones, I. W., et al. (2002). Direct effect of ice sheets on terrestrial bicarbonate, sulphate and base cation fluxes during the last glacial cycle: Minimal impact on atmospheric CO_2 concentrations. *Chemical Geology*, *190*(1–4), 33–44. https://doi.org/10.1016/S0009-2541(02)00109-2

Tranter, M., Sharp, M. J., Lamb, H. R., Brown, G. H., Hubbard, B. P., & Willis, I. C. (2002). Geochemical weathering at the bed of Haut glacier d'Arolla, Switzerland - A new model. *Hydrological Processes*, *16*(5), 959–993. https://doi.org/10.1002/hyp.309

Tranter, M., & Wadham, J. L. (2003). Geochemical weathering in glacial and proglacial environments. In *Treatise on geochemistry* (Vol. 5–9, pp. 189–205). https://doi.org/10.1016/B0-08-043751-6/05078-7

Walker, C. M., Whigham, D. F., Bentz, I. S., Argueta, J. M., King, R. S., Rains, M. C., et al. (2021). Linking landscape attributes to salmon and decision-making in the southern Kenai Lowlands, Alaska, USA. *Ecology and Society*, *26*(1), art1. https://doi.org/10.5751/ES-11798-260101

West, A. J., Galy, A., & Bickle, M. (2005). Tectonic and climatic controls on silicate weathering. *Earth and Planetary Science Letters*, *235*(1–2), 211–228. https://doi.org/10.1016/j.epsl.2005.03.020

Wilson, F. H., Hults, C. P., Mull, C. G., Karl, S. M., & compilers (2015). Geologic map of Alaska. U.S. Geological Survey Scientific Investigations Map 3340, pamphlet 196 p., 2 sheets, scale 1:1,584,000. https://doi.org/10.3133/sim3340

Winnick, M. J., Carroll, R. W. H., Williams, K. H., Maxwell, R. M., Dong, W., & Maher, K. (2017). Snowmelt controls on concentration-discharge relationships and the balance of oxidative and acid-base weathering fluxes in an alpine catchment, East River, Colorado. *Water Resources Research*, *53*(3), 2507–2523. https://doi.org/10.1002/2016WR019724

Young, J. C., Pettit, E., Arendt, A., Hood, E., Liston, G. E., & Beamer, J. (2021). A changing hydrological regime: Trends in magnitude and timing of glacier ice melt and glacier runoff in a high latitude coastal watershed. *Water Resources Research*, *57*(7), e2020WR027404. https://doi.org/10.1029/2020WR027404